2013•2014
FACULTEIT GENEESKUNDE EN LEVENSWETENSCHAPPEN
*master in de biomedische wetenschappen*

# Masterproef

## The role of PREPL in Hypotonia-Cystinuria syndrome; Genetic and immunocytochemical studies

Promotor :
dr. Evi LEMMENS

Promotor :
Prof.dr. JOHN CREEMERS
dr. PHILIP GORDTS

Adelia -

*Proefschrift ingediend tot het behalen van de graad van master in de biomedische wetenschappen*

2013•2014
FACULTEIT GENEESKUNDE EN LEVENSWETENSCHAPPEN
*master in de biomedische wetenschappen*

# Masterproef

## The role of PREPL in Hypotonia-Cystinuria syndrome; Genetic and immunocytochemical studies

Promotor :
dr. Evi LEMMENS

Promotor :
Prof.dr. JOHN CREEMERS
dr. PHILIP GORDTS

Adelia -

*Proefschrift ingediend tot het behalen van de graad van master in de biomedische wetenschappen*

universiteit hasselt | Maastricht University

# Table of Contents

# List of abbreviation

| | |
|---|---|
| APEH | : acylaminoacyl-peptide hydrolase |
| AP-1 | : adaptor protein - 1 |
| Arf-1 | : adenosine diphosphate Ribosylation Factors - 1 |
| Array-CGH | : array comparative genomic hybridization |
| β-ME | : β-mercaptoethanol |
| C2Orf34 | : chromosome 2 open reading frame 34 |
| CAMKMT | : calmodulin-Lysine N-Methyltransferase |
| DMEM/F12 | : Dulbecco's modified Eagle's medium/Ham F-12 |
| DNA | : deoxyribonucleic acid |
| dNTP | : deoxyribonucleotide triphosphate |
| DPPIV | : Dipeptidyl peptidase-4 |
| ECL | : enhanced chemiluminescence |
| EDTA | : ethylenediaminetetraacetic acid |
| ER | : endoplasmic reticulum |
| FCS | : fetal calf serum |
| FP-Biotin | : biotinylated fluorophosphonate |
| GAP | : GTPase-activating protein |
| GDP | : guanosine diphosphate |
| GEF | : guanine nucleotide exchange factor |
| GFP | : green fluorescent protein |
| GTP | : guanosine triphosphate |
| HCS | : hypotonia-cystinuria syndrome |
| HEK293T | : human embryonic kidney 293-T |
| IBMX | : 3-Isobutyl 1-methylxanthine |
| LB | : Luria Bertani |
| LDCV | : large dense core vesicle |
| MEF | : mouse embryonic fibroblast |
| $MgCl_2$ | : magnesium chloride |
| mU6pro | : mouse U6 shRNA promoter |
| N2a | : Neuro2a |
| OpdB | : oligopeptidase B |
| PBS | : Phosphate buffered saline |
| PCR | : polymerase chain reaction |
| PI-4-P | : phosphatidylinositol 4-phosphate |
| PPM1B | : protein phosphatase, $Mg^{2+}/Mn^{2+}$ dependent, 1B |
| PREP/PREPL | : prolyl endopeptidase / prolyl endopeptidase-like |
| qRT-PCR | : quantitative real time PCR |
| RNA | : ribonucleic acid |
| RNAi | : RNA interference |
| RNAPol III | : RNA polymerase III |
| SDS | : sodium dodecyl sulphate |
| SLC3A1 | : solute carrier 3, member 1 |
| shRNA | : short hairpin RNA |
| siRNA | : small interference RNA |
| SOC | : Super Optimal broth with Catabolite Repression |
| TGN | : trans golgi network |

# Acknowledgment

The work of this master thesis would have overwhelmed me had it not been for all the help and support I received along the way. First, I would like to thank God for His blessings. I would also like to express my appreciation to my advisor Prof. John Creemers for giving me the privilege to be a part of his team and make a scientific contribution. Your advice, critics, and trusts have provided me with well rounded academic experience and helped me to develop my independency.

I would also like to thank Siao Hann Then for helping me at the beginning of my internship and Dr. Philip Gordts for his time and assistance in writing thesis. I must also acknowledge people in Lab of biochemical and neuroendocrinology: Krizia, Pieter, Sandra, Jeroen, Luc, and Bas. I am sincerely grateful for your assistance when I encountered difficulties and for your encouragement when I was pessimistic. Thank you for all the stories, humours, entertainment, and food in the lab. I would also like to convey thanks to Dr. Evi Lemmens, for constantly monitoring my progress.

My deepest gratitude is dedicated to my family. Being 8000 miles away does not stop them from loving and supporting me, being there for me when times get rough, and allowing me to be as ambitious as I want. My special appreciation for my boyfriend, Niek. Thank you for being patience, comforting me when I am upset, believing in me, and encouraging me to stand up for myself. Not forgetting my best friend, Brigitta. Thank you for the insightful scientific discussion, and for being a sister to me. Last but not least, I would like to thank my friends all over the world, for providing me with support and friendship.

# Abstract

Hypotonia Cystinuria Syndrome (HCS) is a recessive disease caused by deletion of *SLC3A1* and *PREPL* on chromosome 2p21. HCS patients are commonly characterised by cystinuria type I, neonatal hypotonia, and growth hormone deficiency. The loss of SLC3A1 causes cystinuria type I. However, the functions of PREPL to date are unknown. Previous studies have identified PREPL as an effector of AP-1 which is involved in cargo selection and vesicular trafficking. Overexpression of PREPL redistributes AP-1 in the cytoplasm, while downregulation of PREPL increases AP-1 binding at the TGN. The loss of PREPL also decreases vesicles secretion. Therefore it is hypothesized that PREPL mediates regulated secretion by interracting with AP-1.

In the present study, our research group aimed to increase the current understanding of the pathophysiology of PREPL deficiency through immunocytochemical(ICC) and genetical studies. The ICC studies included optimisation of antibodies, preparation of shRNA and optimising the use of a phogrin-pHluorin construct for monitoring PREPL effects on vesicles secretion by live cell imaging, and co-localisation of AP-1 in TGN by using PREPL KO MEFs.

Firstly, we optimised B01 anti-PREPL that works against mouse and human PREPL, and E9 anti-PREPL that works against human PREPL in immunostaining. In western blot, B01 antibody could only detect human PREPL overexpressed in HEK293T, while E9 could detect endogenous and human PREPL overexpressed PREPL in HEK293T. Both antibodies were unable to detect PREPL expression in βTC-3 and wild-type MEFs in western blot.

Secondly, we developed species-specific shRNA construct that targets PREPL in mouse cells. shRNA efficiency in silencing PREPL in transiently transfected βTC-3 and N2a cells was shown to be 48% and 52%, respectively. This is peculiar since the transfection efficiency checked by ICC was only 13% for βTC-3 and 14% N2a cells. Furthermore, phogrin-pHluorin expression was confirmed by signals at 90 kDa in western blot

We also confirmed the effect of PREPL in AP-1 distribution by MEF cells. Loss of PREPL accumulated AP-1 in TGN. On the other hand, the presence of PREPL in the cells induced AP-1 dispersal in the cytoplasm. This supports our hypothesis that PREPL is involved in vesicles secretion.

In the genetics study, 8 patients were screened for novel deletions in PREPL and one or more of the flanking genes, SLC3A1 and C2Orf34. Four were found to have deletion B, while the rest of the patients have novel deletions. The exact deletion size is still yet to be determined.

Taken together, we optimised several antibodies and developed shRNA against PREPL in mouse that will be useful for further investigating the functions of PREPL. The co-localisation study verified PREPL as effector of AP-1 in regulating vesicles secretion. Nevertheless, more research is necessary to clarify how PREPL deficiency impairs regulated secretion. The genetics study has considerably expanded the repertoire of known HCS alleles and confirmed the relatively high prevalence of the previously reported deletion B in Northern Europe.

# 1. Introduction

Proteases are involved in hydrolizing the peptide bonds in peptides and proteins. This phenomenon is crucial in biological processes such as DNA replication, cell cycle, and apoptosis. Impaired function of peptidases can cause several pathological conditions such as neurodevelopmental disorder. Impaired peptidase activity is mainly caused by modification in the genome. Frequently these modifications are microdeletion, which are smaller than 1Mb and makes them too small to be detected by routine procedures such karyotyping. However, single or multiple genes can be deleted and lead to several recognizable clinical and/or behavioral phenotypes.

Hypotonia-Cystinuria Syndrome (HCS), a microdeletion syndrome, is caused by deletion of multiple genes on chromosomes 2p21 [1]. One of these genes is prolyl-endopeptidase like (PREPL), which is a new member of the serine peptidase family. Interestingly, its biochemical function is unknown. In the present study, we aimed to characterise candidate HCS patients and elucidate the role of PREPL in their clinical manifestations.

### 1.1 Hypotonia-Cystinuria Syndrome

HCS was first described in 1966 as a recessive congenital disorder caused by minor deletions of *SLC3A1* and *Prolyl Endopeptidase–like (PREPL)* [2], [3]. Being a rare disease, only 17 HCS families have been reported to date and are characterised by different deletion sizes. The diagnosis of HCS is easily established when patients feature neonatal hypotonia and cystinuria. In the absence of cystinuria, as in isolated PREPL deficiency, clinical features are too aspecific to make an unambiguous diagnosis.

#### *1.1.1 Phenotype*

HCS has been described to have similar symptoms as Prader Wili Syndrome (PWS). Nevertheless, these 2 syndromes are differentiated by the level of severity of the symptoms. While HCS patients present mild mental retardation and obesity, PWS patients exhibit severe mental retardation and morbid obesity. HCS patients will undergo normal pubertal development and they miss the behavioural problems observed in PWS patients [4].

At birth, HCS patients exhibit generalized hypotonia (decreased muscle tone) shown by the inability to lift the head (Figure 1a). Patients also manifest minor facial dysmorphisms such as dolichocephaly (unproportionally long and narrow head) (Figure 1b), a tented upper lip and ptosis (dropping) of the eyelids as results of the hypotonia (Figure 1c) [5]. Hypotonia may improve with age, even though facial dysmorphism such as ptosis persist throughout life. Mild axial (torso) and proximal (arms and legs) muscle weakness are also observed in several adult patients [4].

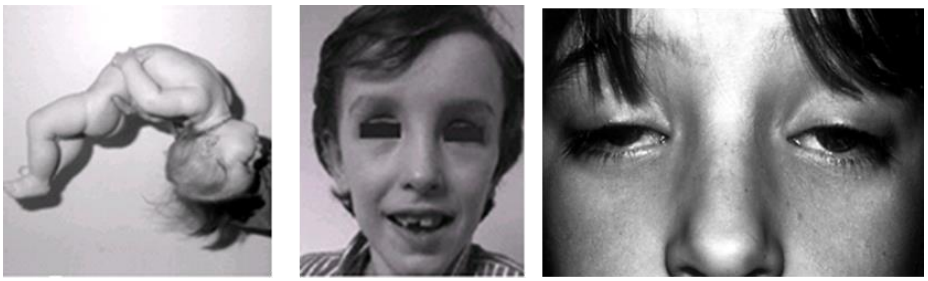


Figure 1. Symptoms shown by HCS patients, including hypotonia (a) [6], dolichocephaly (b) [7], and ptosis (c) [8]

Additionaly, the patients are characterised by growth hormone deficiency and feeding problems that may contribute to failure to thrive. The feeding problem is followed by rapid weight gain, which can eventually lead to obesity. All patients exhibit nasal speech, cystinuria type I, viscous saliva, hypergonadotrophic hypogonadism which is impaired function of gonads causing reduction in testosterone production and increased follicle-stimulating hormone and luteinizing hormone. Around 50% of the HCS patients have learning difficulties [5], [4].

*1.1.2 Genotype*

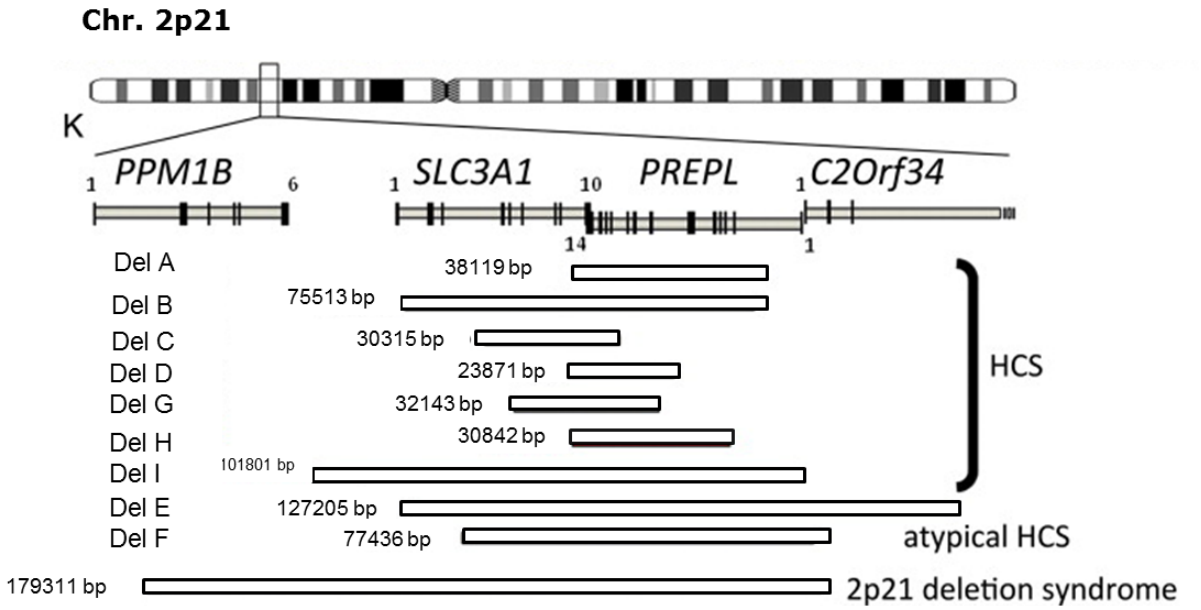


Figure 2. Schematic overview of the genetics involved in HCS and the 2p21 deletion syndrome. Nine different deletions involving *PREPL* and *SCL3A1* ranging from 23.8 kb to 127.2 kb lead to HCS. The additional deletion of *C2Orf34* results in atypical HCS. The absence of PREPL, SLC3A1, C2Orf34, and PPM1B is known as 2p21 deletion syndrome [4].

For HCS, there are 9 different deletions observed on chromosomes 2p21 affecting *SLC3A1* and *PREPL* with deletion sizes that range from 23.8 kb to 127.2 kb (Figure 2). Deletion A, B, C, D, G, H, and I involve the entire or parts of the SLC3A1 and PREPL genes. In addition to deletions in *SLC3A1* and *PREPL*, deletion E includes deletion of the neighbouring *C2ORF34* gene, and deletion F includes the deletion of exon 1 of *C2Orf34* gene. As the start codon ATG is located within exon 1 of C2Orf34, the absence of exon 1 leads to the eliminated expression of C2Orf34. This results in atypical HCS [9].

*1.1.3 Genotype-phenotype correlation*

Cystinuria type 1 is widely known to be caused by deletion of *SLC3A1* (Gene ID: 6519) that encodes the heavy chain of the cystine and dibasic amino acid transporter in the urine tract [10]. It is characterised by excessive cystine in the urine tract, which eventually crystalises into kidney stones. The exact role of *PREPL* in HCS, however, remains elusive.

In atypical HCS, *C2Orf34* is also deleted in addition to *SLC3A1* and *PREPL*. *C2Orf34* (Chromosome 2 open reading frame 34), previously known as *CAMKMT* (Calmodulin-Lysine N-Methyltransferase), is involved in calmodulin methylation [11]. Its deletion in atypical HCS gives additional symptom to classical HCS which is presented by mild to moderate mental retardation.

Furthermore, a bigger deletion of 179 kb involving *SLC3A1*, *PREPL*, *C2Orf34* as well as the *PPM1B* gene is known to cause the 2p21 deletion syndrome. *PPM1B* acts as a phosphatase and is involved in cell cycle and celllular stress response [12]. The phenotypes shown by 2p21 deletion syndrome patients include the phenotypes shown by HCS patients, with the addition of neonatal seizures, hypocalcaemia (low calcium levels) and impaired function of respiratory chain complexes I, III, and V [13].

Table 1. The correlation between deleted gene(s) in HCS, atypical HCS, and 2p21 syndrome and the phenotypes.

| **Deleted gene(s)** | **Phenotypes** |
|---|---|
| SLC3A1 | Cystinuria |
| PREPL | Hypotonia, feeding difficulties, facial dysmorphism, growth hormone deficiency, feeding problem |
| SLC3A1<br>PREPL | Cystinuria, hypotonia, facial dysmorphism Growth hormone deficiency, feeding problem |
| SLC3A1<br>PREPL<br>C2Orf34 | Cystinuria, hypotonia, facial dysmorphism, growth hormone deficiency, feeding problem, mild to moderate mental retardation |
| SLC3A1<br>PREPL<br>C2Orf34<br>PPM1B | Cystinuria, hypotonia, facial dysmorphism growth hormone deficiency, feeding problem, mental retardation, neonatal seizures, hypocalcaemia, impaired respiratory chain |

In atypical HCS and 2p21 deletion syndrome, the complexity and severity of symptoms shown in classical HCS are extended in addition to hypotonia and growth hormone deficiency (table 1). While the loss of SLC3A1 causes cystinuria, *C2orf34* and *PPM1B* are reported to be present in HCS patient. Recently, the first patient with isolated PREPL deficiency has been identified. This patient has a homozygous deletion in PREPL, and develops myasthenic syndrome characterised by feeding difficulties, ptosis, tented upper lips, growth hormone deficiency, and absence of cystinuria [14]. These newly reported results support the hypothesis that *PREPL* deficiency is likely to contribute to hypotonia and growth hormone deficiency observed in HCS [13, 15].

### 1.2 PREPL, a member of the serine peptidase family

The serine peptidase family (S9a) hydrolyses small peptides (30aa) and consists of 4 members. Prolyl endopeptidase (PREP) and oligopeptidase B (OpdB) serve as endopeptidases, while dipeptidylpeptidase IV (DPPIV), and acylaminoacyl-peptidase (APEH) serve as exopeptidases. PREP and OpdB are known to hydrolyze the carboxy terminal of proline and arginine/lysine, respectively. DPPIV on the other hand hydrolyses proline at the penultimate position and APEH will remove acylated amino acids amino terminally [9].

A new member of S9a was discovered and annotated as Prolyl Endopeptidase-like (PREPL) based on its similarity in secondary structure and localisation with PREP [16]. PREPL is predicted to have similar structure as PREP, which is composed of an amino-terminal β-propeller domain and a carboxy-terminal catalytic domain. Despite the similarities between PREP and PREPL, they show striking difference in their amino acid sequence. Both proteins only share 21% similarity in the propeller domain and 37% in the catalytic domain. In addition, PREPL is missing the amino terminal that harbors the catalytic domain which is important in PREP. More importantly, no substrate of PREPL has been found to date [17].

The sequence of PREPL itself contains 14 exons with 2 transcription initiation between exon 1 and 2. This results in 2 isoforms which both are targeted to the cytoplasm [5]. The first isoform is PREPL splice variant 1-4 ($PREPL_{1-4}$) and encodes a ubiquitously expressed 638aa protein referred to as $PREPL_s$. The second isoform is $PREPL_{5-7}$ encoding a 727aa protein. It is referred as $PREPL_L$ and its expression is tissue restricted with it being most abundantly expressed in brain, kidney, and skeletal muscle [5].

#### *1.2.1 PREPL expression*

PREPL is ubiquitously expressed with the highest expression in the brain, including the pyramidal neurons of the neocortex which is important for learning, memory, motor function, and language. At the cellular level, PREPL is localised in the golgi apparatus and the growth cones of neurons [17]. PREPL is also expressed at intermediate levels in skeletal muscle, heart and kidney. The localisation of PREPL expression is consistent with the learning problem and hypotonia in HCS.

#### *1.2.2 Function of PREPL*

As PREPL has the same catalytic triad (Ser, Asp, His) at topologically equivalent position as PREP, a proteolytic activity is expected [9]. The catalytic machinery of PREPL is shown to be active based on its covalent binding of the activity based probe fluorophosphate (FP)-biotin to its serine residue. However the main function(s) of PREPL are still unknown to date[15]. Based on several symptoms occuring in HCS such as growth hormone deficiency and hypotonia, and its inaccellular localizaton, it is assumed that PREPL is involved in the regulated secretory pathway.

### 1.3 Protein transport via exocytosis

The dynamics of molecular transport into and out of cells is regulated via endocytosis and exocytosis, respectively. In endocytosis, extracellular molecules can be internalised into the cells by engulfment (phagocytosis), engulfment of dissolved or liquid materials (pinocytosis) and receptor-mediated endocytosis [18]. Our preliminary studies in the endocrine mouse insulinoma

cell line βTC-3 show that *PREPL* knockdown decreases the regulated secretion of large dense core vesicles (LDCVs) that carry neuropeptides, hormones, and growth factors. These findings suggest a role for PREPL in regulated secretion and are consistent with the growth hormone deficiency observed in HCS patients. In the next paragraph we will discuss the process of exocytosis in more detail.

*1.3.1 Exocytosis*

Exocytosis involves the secretion of molecules such as proteins out of the cells. The N-terminus of translated proteins that contain a signal peptide is recognised by the signal recognition particle (SRP). This interaction results in directing further translation of the proteins into the endoplasmic reticulum (ER), which allows the proteins to be properly folded by chaperones as well as being chemically modified. These modified proteins either stay in the ER or are packed into transport vesicles and shuttled to the golgi apparatus for further maturation. Protein–containing transport vesicles first enter the *cis* face of the golgi network and travel through stacks of membrane sacs called cisternae. As the proteins pass cisternae, they undergo several modification such as additon of sugars (glycosylation), additon of sulphate groups (sulphation), and phosphate groups addition (phosphorylation). Proteins are then sorted into clathrin-coated secretory vesicles for transport to various targets such as plasma membrane, endosomes, and lysosomes, and exit through the *trans* face of the golgi network (TGN) [19]. This secretory pathway can be divided into two parts, the constitutive and regulated pathway. In the former pathway, proteins are secreted continuously. In the regulated pathway, on the other hand, the proteins are stored in the secretory vesicles that are only released upon receiving an extracellular signal (Figure 3) [20].

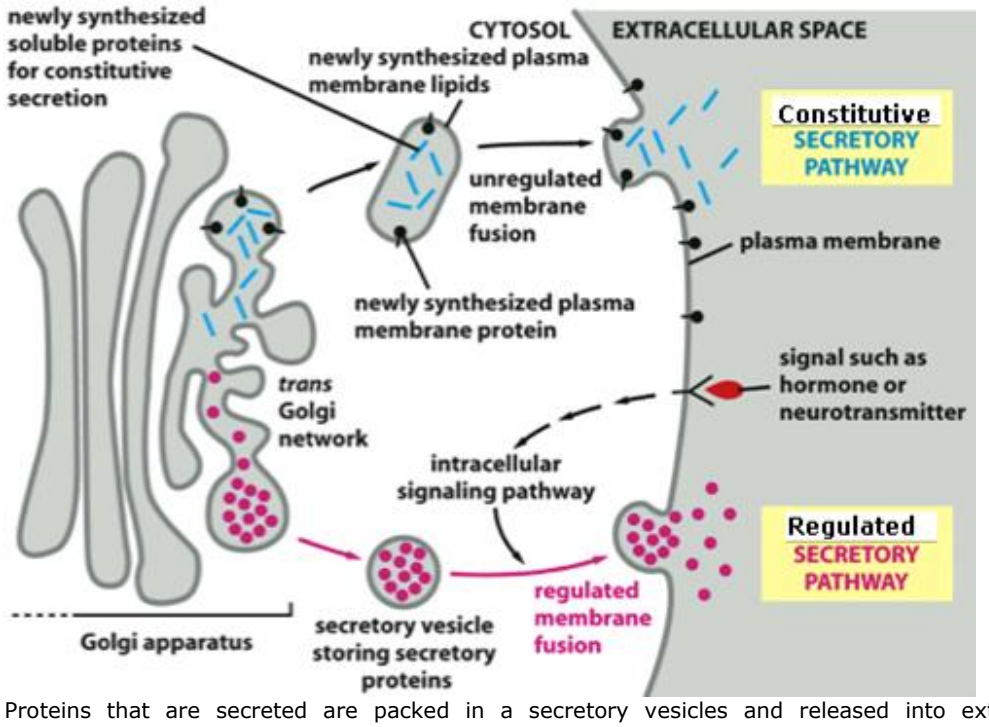


Figure 3. Proteins that are secreted are packed in a secretory vesicles and released into extracellular environment. This is done either via the constitutive secretory pathway, where proteins are secreted continuously, or the regulated secretory pathway, where proteins are secreted upon receiving stimuli from secretagogue. Image adapted from "Molecular Cell Biology, 5th Ed" [21]

*1.3.2 Transport vesicles*

Neurons, endocrine and neuroendocrine cells are cell types which also release proteins by regulated secretion. Large dense core vesicles (LDCVs) are found within these cells. Morphologically, LDCVs are seen as large vesicles containing aggregated hormones and neuropeptides. After being stimulated by a secretagogue, LDCVs release their cargo and recylced back to the Golgi apparatus. Small synaptic vesicles are also involved in regulated secretion in neurons. They contain neurotransmitter and recycled locally following the cargo release [22], [23].

After budding from the TGN, the vesicels undergo maturation. This involves removal of the clathrin-coat, acidification of the membrane, fusion with the plasma membrane, and eventually release of cargo proteins. There are 3 known mechanism for cargo release. The first mechanism is kiss and run, in which vesicles and plasma membrane are not fused completely, resulting in incomplete cargo release. In the second mechanism, however, vesicles and membrane are fused completely, allowing entire cargo to be released [23], [24]. The third mechanism is by releasing intact exosomes, which are endocytic-derived microvesicles found in multivesicular bodies. The exosomes are released into the extracellular environment by fusion of multivesicular bodies with the plasma membrane [25].

In both endocytosis and exocytosis, clathrin-coated vesicles are one of the most essentials components involved in protein transport. The biogenesis of clathrin-coated vesicles, such as budding off the TGN, vesicles cargo selection, and recruiting proteins associated with vesicles organization, is supported by adaptor protein complex (AP). Three isoforms of AP in mammals have been known to date are AP-1, AP-2, and AP-3, in which each of them consists of γ, β, μ, and σ adaptins [26], [27]. The protein transport between TGN and endosomes is mediated by AP-1 [28]. High-affinity binding of AP-1 to plasma membranes calls for a cargo protein with a cytoplasmic domain carrying a tyrosine- or dileucine-based AP-1 binding/sorting motif [29], [30]. Small GTP-binding protein Arf-1 and phosphatidylinositol 4-phosphate (PI-4-P) are also required in membrane binding and vesicles coat formation. Absence of one of the required components leads to failure of AP-1 binding to the membrane and thus impairs protein export from the TGN[31].

*1.3.4 Interaction between PREPL and AP-1*

Through yeast-2-hybrid with AP-1 as a bait, Radhakrishnan, K., et al [31] were able to detect PREPL as one of its binding partner. This binding was confirmed through co-locolisation studies in mouse embryonic (MEF) and human fibroblast, and HeLa Cells. Overexpressing PREPL in MEF cells decreases AP-1 on TGN area, while PREPL deficiency in human fibroblast and HeLa cells increases AP-1 on TGN area. Interestingly PREPL itself also contains the tyrosine- or dileucine-based AP-1 binding/sorting motifs. These preliminary findings, together with symptoms shown by HCS patients (hypotonia and growth hormone deficiency), lead to the hypothesis that PREPL is involved in regulated secretion.

**1.4 Experimental approach**

HCS is a rare disease as it requires deletions of both *PREPL* and *SLC3A1*. Since our original description of HCS in 2006, a total of 25 patients have been diagnosed. Treatment of PREPL

deficiency symptoms is currently limited and only symptomatic. It consists of growth hormone replacement therapy, gavage feeding and behavioral corrections to prevent excessive weight gain. Preventive treatment is also given to avoid kidney stone development. Unfortunately, no treatment exists for the hypotonia, although pyridostigmine has recently been found to provide transient relieve in young patients [14]. Delineating the role of PREPL in regulated secretion will form the essential backbone for further research, such as the molecular mechanism behind its function. It is anticipated that these results will improve the treatment of HCS patients to ease the hypotonia and hopefully target the treatment of a larger group of diseases with similar symptoms as HCS.

As already mentioned, our preliminary studies in the endocrine cell line βTC-3 showed that *PREPL* knockdown decreases the regulated secretion of LDCVs that carry neuropeptides, hormones, and growth factors. This finding supports a role for PREPL in regulated secretion and is consistent with the growth hormone deficiency observed in HCS patients. In this study, we aim to characterise the role of PREPL in regulated secretion as well as identify HCS candidate patients with novel deletion.

### *1.4.1 shRNA and phogrin-pHluorin optimisation*

To analyse the influence of PREPL deficiency in mouse insulinoma cell line βTC-3 by live cell imaging, constructing shRNA that targets PREPL in mouse cells and confirming the expression of phogrin-pHluorin, a pH sensitive-GFP [32] in the construct are necessary to be done. When both are optimised, βTC-3 cells will be co-transfected with small hairpin RNA (shRNA), which will knockdown PREPL, and a phogrin-pHluorin construct to monitor vesicular trafficking. Subsequently, the effect of PREPL deficiency in the amount and time course of LDCVs secretion, as well as vesicles fusion to plasma membrane will be observed by live cell imaging.

### *1.4.2 Colocalisation study: PREPL as an effector of AP-1*

Recently, it was reported that PREPL mediates the release of clathrin associated with AP-1 from the TGN in mouse embryonic and human fibroblasts [31]. It was shown that loss of PREPL led to a more intense and bigger TGN area in patient's fibroblast, while it led to a more intense but less spread out TGN are in HeLa cells with PREPL knockdown. We would like to confirm this result in patient's fibroblast and mouse fibroblast with PREPL knockout. The effect of PREPL deficiency on PREPL mediated AP-1 release from TGN will be visualised by confocal microscopy.

### *1.4.3 Patient study; characterising novel deletion*

Characterising HCS patients clinically has been quite challenging due to several factors. As they are diagnosed in the features of cystinuria and hypotonia, isolated PREPL deficiency shows aspecific features to make an explicit diagnosis. This is due to the fact that the symptoms shown are overlapping with other disorders that are also characterised by hypotonia, such as the Prader Wili Syndrome. Moreover, since HSC is a recessive trait, HCS carriers are usually asymptomatic. In order to characterise HCS patients and/or carriers, as well as identifying novel deletion, molecular approaches are preferred.

In the present study, samples of HCS candidate patients were retrieved from several hospitals in Belgium and Italy. Symptoms of each patient are varied with some show imperceptible HCS phenotypes. Nevertheless, the array comparative genomic hybridisation (arrayCGH) results of

some patients show deletion of SLC3A1 and PREPL, which correlates with HCS. Using quantitative polymerase chain reaction (qPCR), the size of the deletion will be determined in order to set the exact breakpoints region and establish the correlation between deleted genes, deletion size, and phenotypes.

# 2. Materials and methods

## 2.1 Cloning

### *2.1.1 Nucleotides sequencing*

Previously made shRNA construct targetting human PREPL was sequenced using ABI Prism Big Dye Terminator Cycle Sequencing Ready Reaction Kit (Applied Biosystem, USA). The reaction mix was prepared by mixing 2 µl Bigdye TRRmix, 6 µl ABI dilutioner (200 mM Tris pH9, 5 mM $MgCl_2$), 10 µl $H_2O$, 1 µl of DNA (1 µg/µl), and 1 µl primer (5 pmol/ µl). The PCR conditions were 3 minutes 96$^{o}$C; 25 cycles of 10 seconds 96$^{o}$C, 10 seconds 55 $^{o}$C, 2 minutes 60 $^{o}$C. The PCR products were purified by incubation with 125 mM EDTA and 100% EtOH for 15 minutes. Samples were precipitated with Ethanol 70%, dissolved in HiDi formamide and denatured at 95$^{o}$C for 3 minutes. The sequencing results were obtained by ABI Prism 3100 Genetic Analyzer and analysed by Vector NTI 8.0.

### *2.1.2 Constructing PREPL shRNA primer directed against mouse cells*

The shRNA sequence obtained were checked for their specificity for the target gene by means of homology search in mouse database with the help of NCBI blast. The sense primer consisted of 19 nucleotides of shRNA target sequence followed by 9 nucleotides forming a loop, and 19 antisense nucleotides that were complementary to the 19 sense nucleotides. At the 5' end of the sense primer, 3 T's were added to create a BbsI restriction site. At the 3' end, TTTTTT (termination signal for RNApolIII) and GGAA were added. At the 5' end of the antisense primer, GATCTTCCAAAA were added to create BamHI restriction site. At the 3' end, a C was withdrawn to create complementary double – stranded DNA. All primers were synsthesised by Eurogentec, Belgium.

### *2.1.2 Primers annealing*

Annealing mixture was prepared by combining 20 µl of forward and reverse primers (0.25 nmol/µl) with 5 µl of $H_2O$ and 5 µl of 10x siRNA annealing buffer (1M NaCl, 100nM Tris pH 7.4). The annealing oligos were heated at 95$^{o}$C for 10 minutes, and cooled down until 37$^{o}$C in order to create double-stranded oligonucleotides

### *2.1.3 Vector digestion and purification*

In total of 50 µl, 5 µg of vector, 1 U/µl of restriction enzyme (2 µl BamHI and 2 µl BbsI), 5 µl 10x restriction buffer, and $H_2O$ were added. The digestion solution was incubated at 37$^{o}$C for 1-2 hours. To digested vector, 1x loading buffer was added and mixture was run on 1% agarose gel. The largest band in size containing digested vector was cut and purified using Wizard DNA clean up (Promega, USA)

### *2.1.4 Double-stranded DNA ligation in vector*

The oligonucleotides were diluted to 1/4000 in 0.5x shRNA annealing buffer. A mixture of 2 µl T4 ligase, 2 µl 10x ligation buffer, 2 µl digested vector, and 14 µl of annealed oligos was prepared and incubated at room temperature for 2 hours.

### *2.1.5 Electroporation*

The shRNA construct were resuspended in XL-1 blue competent cells. Electroporation was performed by applying electricity pulse of 2500 Volts/cm to shRNA and competent cells mixture. The mixture was incubated in SOC medium (2% trypton, 0.5% yeast extract, 8.5 mM NaCl, and 2.5 mM KCl, 10 mM $MgCl_2$, 0.36% glucose, pH7) for 1 hour at 37$^{o}$C. Subsequently, the cells were innoculated on Luria Bertani (LB) (1% trypton, 0.5% yeast extract, 170 nM NaCl) plate with proper antibiotics (Ampicillin 1µl/ml) and grown overnight at 37$^{o}$C.

### *2.1.6 Plasmid DNA isolation from bacteria (Miniprep)*

Colonies grown on LB plate were picked and cultured in 5 ml LB medium with ampicillin at 37$^{o}$C overnight. The mini prep procedure was conducted based on Plasmid DNA Purification Kit Nucleobound AX$^{R}$ (Macherey Nagel, Germany). The yielded DNA were dissolved in TE buffer (10 mM Tris-HCl and 1 mM Ethylenediaminetetraacetic acid (EDTA), pH 8.0) and sequenced.

### *2.1.7 Plasmid DNA isolation from bacteria (Maxiprep)*

From the bacteria culture used for miniprep, 0.5ml was stored in glycerol stock at -80$^{o}$C, and 1 ml was cultured in 150 ml LB medium with suitable antibiotics (ampicillin) and grown overnight at 37$^{o}$C. The DNA was isolated from the bacteria according to the materials and instructions of Plasmid DNA Purification Kit Nucleobound AXR from Macherey Nagel, Germany. The yielded DNA was dissolved in TE buffer pH 8.0

## 2.2 Cell culture

### *2.2.1 Cells preparation for Immunofluorescence and Western blot*

MEF cells with PREPL Knockout (KO), MEF wild-type (WT), HEK293T and βTC3 cells were washed with Versene (Gibco Life Science, UK) prior cell detachment by trypsin. HEK293T and βTC3 cells were resuspended in medium containing DMEM/F12 (Gibco Life Science. UK) with 10% fetal calf serum (FCS), while MEF cells were resuspended with addition 1/100 pen/strep into the afore mentioned medium. The cells were split and grown on coverslip glass in 24-wells plates for immunofluorescence and 6-wells plates for western blot at 37°C in a 5% $CO_2$ incubator.

### *2.2.2 Transfection with xTremegene or Turbofect*

HEK293T cells were transfected with a eukaryotic construct expressing human PREPL in a 10 cm$^2$ plate. Six µl of xTremegene transfection reagents (Roche, USA) was added to 200 µl DMEM/F12 with 10% FCS. After 5 minutes at room temperature, 2 µg of DNA was added. The mixture was incubated at room temperature for 30 minutes before applied to the cells. Other cells were transfected in a 10 cm$^2$ plate with 4 µg of DNA mixed with 8 µl of turbofect added to 400 ml of DMEM/F12. The mixture was incubated at room temperature for 20 minutes before adding to cells. For cell transfection in 2.5 cm$^2$ plate, the amount applied was ¼ of that in 10 cm$^2$ plate.

### *2.2.4 Immunofluorescence*

PREPL KO MEFs, MEF WT, and βTC3 cultured on coverslip glass in 24-well plates were quenched with solution containing phosphate buffered saline (PBS) (Gibco Life Science, UK) and 0.25g/100ml NH4Cl. The cells were then blocked in block buffer (1M Tris/HCl pH7.4, 5M NaCl, Block reagent) with 0.2% Triton and incubated with PREPL primary antibodies (Table 2) diluted in block buffer.

The cells were rinsed with PBS and 0.2% Triton preceding incubation in the dark with secondary antibodies (Table 2) diluted in block buffer. Cells were mounted using vectashield (vector laboratorium, USA) with DAPI.

Table 2. Primary and secondary antibodies used in immunofluorescence

| **Primary antibody** | **Secondary antibody** |
|---|---|
| 1/100 Mouse anti hPREPL (B01, Abnova, USA) | 1/500 Goat anti mouse (A11001, Invitrogen, USA) |
| 1/50 Mouse anti hPREPL (E9, Santa Cruz, USA) | |
| 1/250 Mouse anti adaptin γ (AP-1) (A36120, BD transduction lab, USA) | |
| 1/200 Mouse anti human TGN46 (ab16059, Abcam, UK) | 1/500 Goat anti Rabbit (A11008, Invitrogen, USA |

**2.3 RNA extraction and cDNA synthesis**

Cells were collected in PBS, and centrifuged at 1000 rpm for 10 minutes, $4^0$C. Pellets were used for RNA extraction using a NucleoSpin RNA II kit (Macherey Nagel, Germany). Cells were lysed with 350 µl RA1 and β-mercaptoethanol. The binding of RNA onto silica membrane was performed by adding 70% EtOH. Membrane desalting buffer was applied, followed by 10 µl reconstituted rDNase and 90 µl reaction buffer rDNase to digest DNA for each lysate. The reaction mix was incubated at room temperature for 15 minutes, followed by addition of RA2 buffer. Silica membrane was washed by RA3 buffer and the DNA was eluted by RNase-free $H_2O$ and stored at -$80^o$C. cDNA synthesis was performed using the iScript cDNA synthesis kit (Bio-Rad, USA) accoriding to the manufacturer's instructions. cDNA was diluted 1/8 for qPCR

**2.4 Western blot**

Cells were collected in sample buffer (10%Sodium dodecyl sulphate (SDS), 2% glycerol, 0.5M Trisbuffer pH6.8, $H_2O$) and sonicated. β-mercaptoethanol was added into the cells before heating the samples for 10 minutes at 65°C. Proteins were separated by running the lysates in 7% Tris-acetate SDS gel (Invitrogen, USA) and transferred to the nitrocellulose blot membrane. The blots were blocked with either milk buffer (5% milk, PBS, 0.2% triton) or standard buffer (Block buffer, 0.2% triton). Subsequently, blots were incubated in primary antibodies (1/1000 mouse anti-mouse PREPL (B01, Abnova, USA) or 1/1000 mouse anti human PREPL (E9, Santa cruz, USA)) diluted in corresponding milk or standard buffer before washing with PBS and 0.2% triton. Blots were incubated with secondary antibodies (1/2000 rabbit anti mouse (Dako, Denmark)) and washed with PBS and 0.2% triton. ECL detection reagents containing Luminol enhancer solution and peroxide solution (1:1) was applied on the blot before visualisation by CCD Camera (ImageQuant LAS 4000. GE Healthcare Life science, UK).

## 2.5 Mutation analysis of patient's genomic DNA

### *2.5.1 Primer design*

Nucleotide sequences were obtained from Ensembl Gene ENSG00000138078, ENSG00000138079, and ENSG00000143919 for PREPL, SLC3A1, and C2Orf34, respectively. The primers for deletion screening were made using Probe Finder (Roche).

### *2.5.2 Patients*

This study was approved by the Institutional Review Boards of the Hospitals of Leuven University. Informed consent was retrieved from patients or their parents. Genomic DNA samples of patients were derived from anonymous persons performing clinical diagnostics in the corresponding hospitals, and were used for deletion screening by qPCR.

### *2.5.3 Quantitative Polymerase Chain Reaction (qPCR)*

qPCR was conducted by preparing 15 µl mix of mastermix (Bio-Rad, USA); containing polymerase, dNTP, buffer, SYBR green fluorescent; primer mix (2.5 µM Forward primer and 2.5 µM Reverse primer. Eurogentec, Belgium), $H_2O$, and 5ng/µl cDNA. The qPCR run condition is stated in table 3.

Table 3. qPCR condition

| | **Cycle 1** | **Cycle 2: 40x** | | **Cycle 3** | **Cycle 4** | **Cycle 5: 81x** | **Cycle 6** |
|---|---|---|---|---|---|---|---|
| **Step** | 1 | 1 | 2 | 1 | 1 | 1 | 1 |
| **Temperature** | 95°C | 95°C | 60°C | 95°C | 55°C | 55°C | 20°C |
| **Time** | 10:00 | 0:15 | 1:30 | 1:00 | 1:00 | 0:06 | Hold |

### *2.5.4 Quantification of qPCR*

SYBR green is beamed through double helix DNA at 497nm, emitting fluorescent that is depicted in amplification plot. The more the DNA amplifies, the higher the intensity of the fluorescent. The quantification is conducted based on difference in threshold-cycle values (CT), which reflects initial amount of DNA template used. The amount of allele is calculated by Livak-method. In this method, the expression of target gene depicted through CT values is normalized to that of endogenous reference gene, giving a ΔCT value. This normalization is further normalised to healthy control (calibrators) to give a ΔΔCT value, resulting in the amount of alleles of target genes ($2*2^{(-\Delta\Delta CT)}$). The presence of aspecific dsDNA (primer dimers and aspecific products) can be verified with melt curve that changes in fluorescent signal and thus giving 2 peaks (Figure 4)

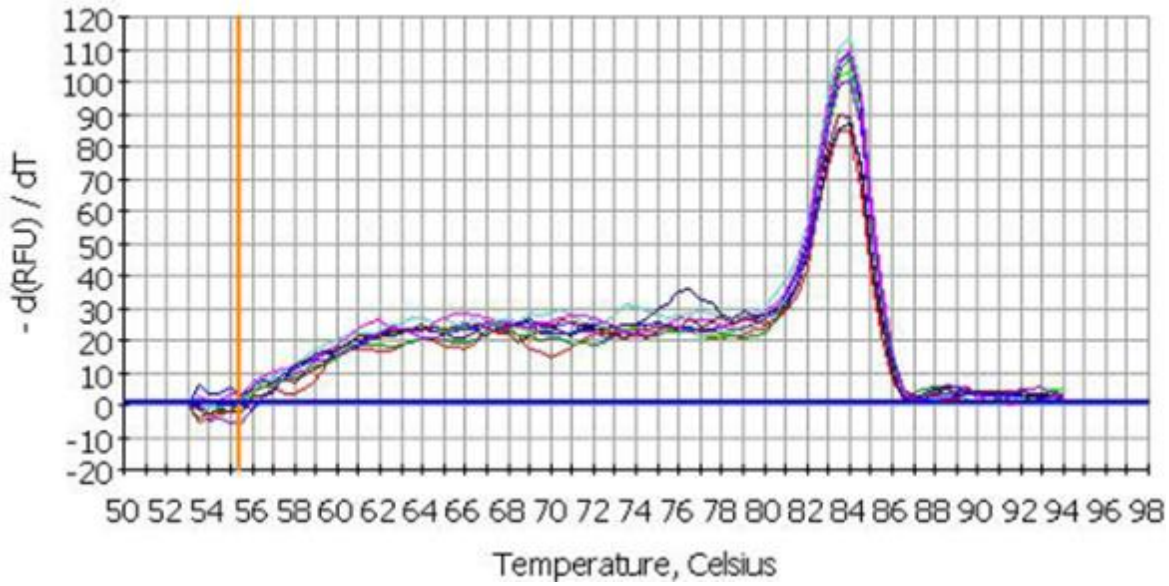


Figure 4. Melt curve shown in QPCR. The presence of only 1 sharp peak instead of 2 or more shows the specificity of the amplification [33]

### *2.5.5 Junction-fragment Polymerase Chain Reaction (PCR)*

PCR was prepared in a total volume of 25 µl containing 10dNTP mix, Buffer – $MgCl_2$, enhancer, $MgCl_2$, 1 unit (U) Taq polymerase, 12.5 pmol of each primers (Eurogentec, Belgium), and 1 µl of DNA. The PCR conditions were 1 minutes 95°C; 10 cycles of 30 seconds 95°C, 1 minute 65°C, and 1 minute 72°C; 25 cycles of 30 seconds 95°C, 1 minute 55°C, and 1 minute 72°C; with a 7 minutes 72°C.

# 3. Results and Discussion

### 3.1 PREPL Antibody Validation and optimalization

To check the expression of PREPL in cells and the effect of PREPL deficiency in cells, we will use several techniques such as immunocytochemistry, western blot, and qPCR. The former two techniques required antibody binding to PREPL for visualisation. Therefore several available antibodies targeting PREPL needed to be validated and optimised for the respective assays.

The lab of Prof. Creemers previously developed 3 rabbit PREPL polyclonal antibodies. The first anti-PREPL antibody was generated against a specific peptide sequence in PREPL and had been purified before. The other two antibodies were generated against the entire PREPL sequence and had not been purified. The serum from the rabbits were obtained before immunisation with human PREPL, 40; 70; and 100 days post immunisation. Besides the antibodies developed by our lab, 2 commercial mouse anti PREPL antibodies provided by Abnova (B01) and Santa Cruz (E9), and 1 commercial rabbit anti PREPL antibodies provided by Biorbyt (orb35859) were also validated and optimised. The antibodies sensitivity and specificity were tested by immunostaining and western blot using HEK293T, βTC-3, as well as mouse embryonic fibroblast (MEF) cells that were obtained from both wild-type and PREPL knock out (KO) mice.

Immunostaining results from homemade rabbit polyclonal anti-PREPL and commercial rabbit anti-PREPL (orb35859) antibodies showed intense punctuated PREPL staining especially in HEK293T and βTC-3 cells. However, these antibodies gave non-specific binding as PREPL KO MEF cells (not expressing PREPL), showed similar affinity to the rabbit anti-PREPL antibodies (Figure 5a). These results were confirmed by western blot, as use of the antibodies showed the presence of several aspecific bands at various sizes (Figure 5b).

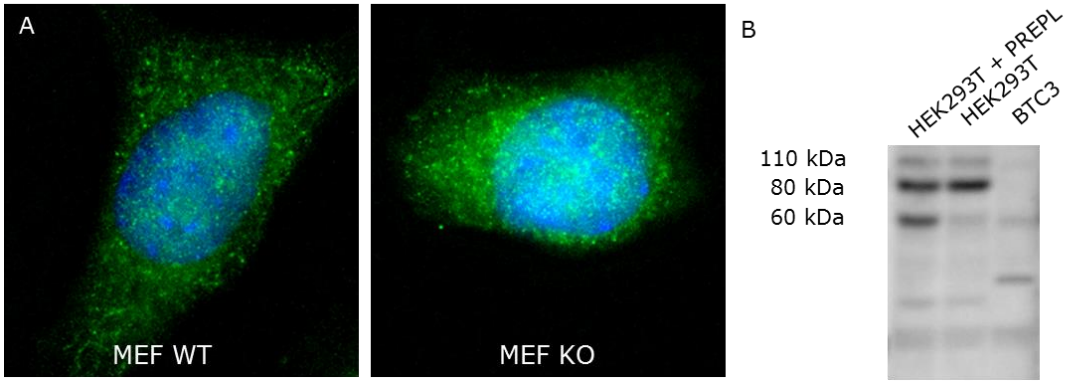


Figure 5. Representative data from homemade rabbit polyclonal anti-PREPL. Aspecificity of antibodies is shown by: (a) immunostaining of MEF WT and PREPL KO MEFs and (b) presence of non specific bands in western blot using HEK293 cells overexpressing PREPL, HEK293 cells and BTC-3 cells.

Meanwhile, anti PREPL antibody (B01) showed strong affinity towards endogenous PREPL expressed by MEF wild-type (Figure 6a), βTC-3 (Figure 6c), and in HEK293T cells (Figure 6d). No signal could be detected when using this antibody in PREPL KO MEFs (Figure 6b). The commercial mouse anti-PREPL antibody (E9), on the other hand, showed great affinity towards PREPL in

HEK293T cells (Figure 6e), but no signal could be detected in mouse cell lines (βTC-3 and MEF wild-type). Different results were obtained when using the commercial antibodies for western blot (Figure 6f). Interestingly, the B01 antibody only detected human PREPL when it is overexpressed in HEK293T cells in this application with no signal from endogenous PREPL when using lysates from HEK293T cells, MEFs and PREPL KO MEFs. The E9 antibody did detect both endogenous and overxpressed human PREPL in HEK293T cells but was unable to detect mouse PREPL (Figure 6f). No aspecific bands were deteted when using both commercial antibodies on western blot.

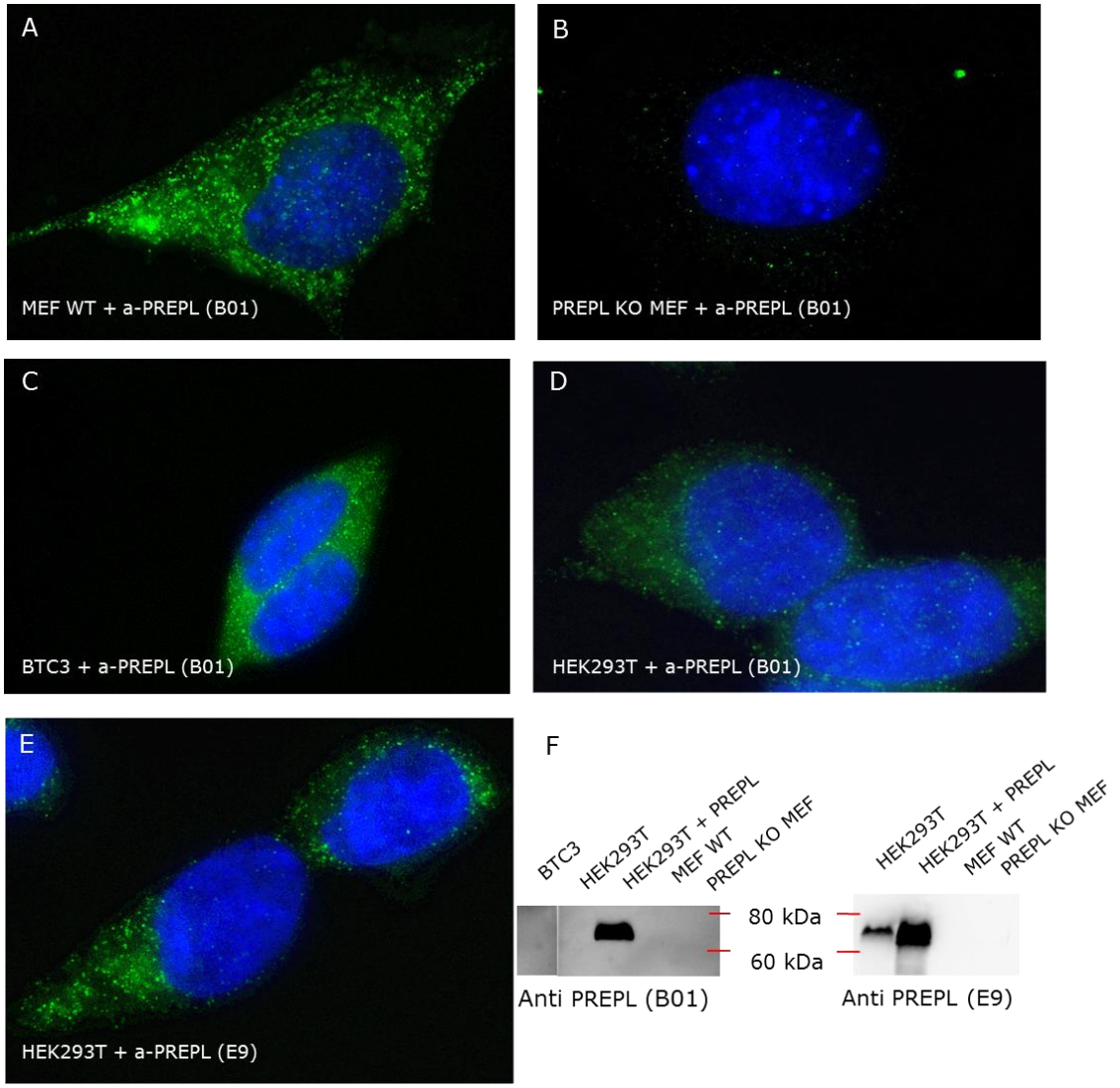


Figure 6. PREPL expression in MEF wild-type (A), MEF with PREPL knockout (B), βTC-3 (C), and HEK293T (D) as detected by PREPL antibody (B01). PREPL expression in HEK293T was also detected by PREPL antibody (E9) (E). The sensitivity and specificity of both commercial antibodies were also observed in western blot shown by bands at approximately 75 kDa for PREPL (F). B01 antibodies shows PREPL expression in HEK293T with PREPL overexpression, while E9 antibody shows that in both HEK293T with and without PREPL overexpression.

Both commercial antibodies are generated against human PREPL protein. Different affinity towards mouse and human cells shown by mouse anti-PREPL (B01) and mouse anti-PREPL (E9) antibodies can be explained by the clonality of the antibodies. Mouse anti-PREPL antibodies (B01) are polyclonal antibodies, and are predicted to have affinity for PREPL from both mouse and human cell

lines and tissues. Mouse anti-PREPL antibodies (E9), on the other hand, are monoclonal antibodies, allowing them to bind only to PREPL protein in human cells. Both commercial antibodies were also used to visualise PREPL expression in parafin-embedded brain tissues from wild-type and PREPL knockout mice. Despite different antibodies concentration was tested from 1/200, 1/250, 1/100, 1/50, and 1/25, PREPL could not be detected in brain tissues from wild-type mice (data not shown). The data therefore suggest that both antibodies are not appropriate for fixed frozen tissues.

### 3.2 Optimisation of shRNA and phogrin-phluorin for analysing exocytosis by live cell imaging

As PREPL is hypothesised to be involved in regulated secretion, we attempt to visualise the motion of LDCVs in βTC-3 cells with PREPL knockdown. For this study, βTC-3 cells will be co-transfected with shRNA to downregulate PREPL expression, phogrin-pHluorin to monitor the LDCVs exocytosis, and internal fluorescent marker to indicate single cells with PREPL knockdown. Several preparations were therefore required prior visualisation by live cell imaging.

#### *3.2.1 Development of a shRNA targeting murine PREPL*

In order to investigate the effect of PREPL deficiency in mouse βTC-3, PREPL expression in βTC-3 will be silenced. Several gene silencer methods such as siRNA and shRNA were considered. siRNA is obtained by vitro synthesis which is a simple and rapid method, and is delivered directly into the cytosol. siRNA is not synthesised by the host machinery and the concentration of siRNA decreases in culture as the cells divide. This characteristic of siRNA allows only limited silencing duration times, and was not feasible for long term knockdown. The shRNA approach, on the other hand, is introduced into the cells by either plasmid or viral vector. As opposed to siRNA, shRNA is continuously synthesised in the nucleus by the host machinery. This will give a more durable silencing of the target gene compared to siRNA [34].

The lab of Prof. Creemers previously developed a shRNA construct in mU6pro plasmid targeting human PREPL and but not for murine PREPL. In order to develop a shRNA that targets murine PREPL, we sequenced the construct targeting human PREPL to obtain PREPL and hairpin sequence in the shRNA. This PREPL sequence was compared to murine PREPL by NCBI Blast. The results revealed 2 nucleotides mismatches between the murine and human PREPL sequence. New primers with murine PREPL sequence were designed in order to silence PREPL in mouse derived cells. The basic pattern of shRNA primers is as follows:

- Sense oligonucleotides
  5’-TTTNNNNNNNNNNNNNNNNNNNTCTCTTGAANNNNNNNNNNNNNNNNNNNTTTTTTGGAA-3’

- Antisense oligonucleotides
  5’-GATCTTCCAAAAAANNNNNNNNNNNNNNNNNNNTTCAAGAGANNNNNNNNNNNNNNNNNNN-3’

- shRNA target sequence
  sense: 5’ GCTGACAGTGATAATTATG 3’

antisense: 5′ CATAATTATCACTGTCAGC 3′

- Double-stranded oligonucleotides

| | BbsI | Sense strand | Loop | Antisense strand | RNA Pol III Terminator | BamHI |
|---|---|---|---|---|---|---|
| 5′ | TTT | GCTGACAGTGATAATTATG | TCTCTTGAA | CATAATTATCACTGTCAGC | TTTTTTGGAA | 3′ |
| 3′ | | GACTGTCACTATTAATAC | AGAGAACTT | GTATTAATAGTGACAGTCG | AAAAAACCTTCTAG | 5′ |

The double-stranded oligonucleotides were cloned in mU6pro vector by means of a BbsI and BamHI digestion prior to ligation. Positive ligated clones were verified by sequencing analysis (data not shown).

### *3.2.2 Testing shRNA efficiency for murine PREPL silencing*

The efficiency of shRNA construct in silencing PREPL was evaluated by qPCR for PREPL gene expression in βTC3 and N2a cells. Neuro2a (N2a) cells, i.e. a mouse neuroblastoma cell line expressing PREPL (Figure 7), were used as a positive control. Experiments were performed 48 hours after transfection with Turbofect.

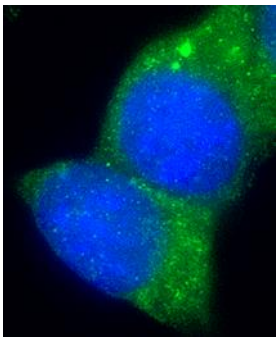

Figure 7. PREPL expression in N2a

Transfection efficiency was monitored by co-transfecting βTC3 and N2a cells with mouse PREPL shRNA construct together with a phogrin-GFP. The cells were fixed and stained with mouse anti PREPL antibodies (B01) followed by goat anti mouse Alexa-fluor 555 for the secondary antibody. Transfection efficiency was calculated from percentage of cells expressing GFP signal that was preserved post cells fixation.

By comparing the amount of PREPL expression by qPCR between mock-transfected and shRNA construct transfected cells, it was shown that the shRNA construct was able to knockdown approximately 48% and 52% of PREPL in βTC3 and N2a cells respectively (Figure 8a). However, the transfection efficiency checked by immunostaining showed that only 13% of βTC3 cells and 14% of N2a were successfully transfected (phogrin-GFP positive cells) (Figure 8b, c and d). Despite low transfection efficiency, the shRNA seems to have a high knockdown efficiency for PREPL gene expression. As the cells were prepared in different volume which are 6-wells plate for qPCR and 24-wells plate for immunostaining, this condition made it not suitable for comparison. Ideally, the cells are prepared on 24-wells plate for both techniques to make the results more compatible. Moreover,

the cells for immunostaining were co-transfected with 2 constructs i.e shRNA and GFP, while they were transfected only with shRNA for qPCR. It is plausible that co-transfecting the cells with 2 construct might influence overall transfection efficiency. Also some cells that were negative for phogrin-GFP might have still been transfected with the shRNA construct and vice versa. To further validate this, it is essential to transfect the cells with single constructs and validate them by fluorescence-activated cell sorting (FACS) to allow better sorting of cells with PREPL knockdown or phogrin-GFP, and transfection efficiency quantification. Validation of different tranfection protocols to optimise transfection efficiency is necessary as well. Finaly, we can have over- or underestimated our transfection efficiency as we have not determined the protein stability of Phogin overexpression as well its effects on cell survival in the cell types used.

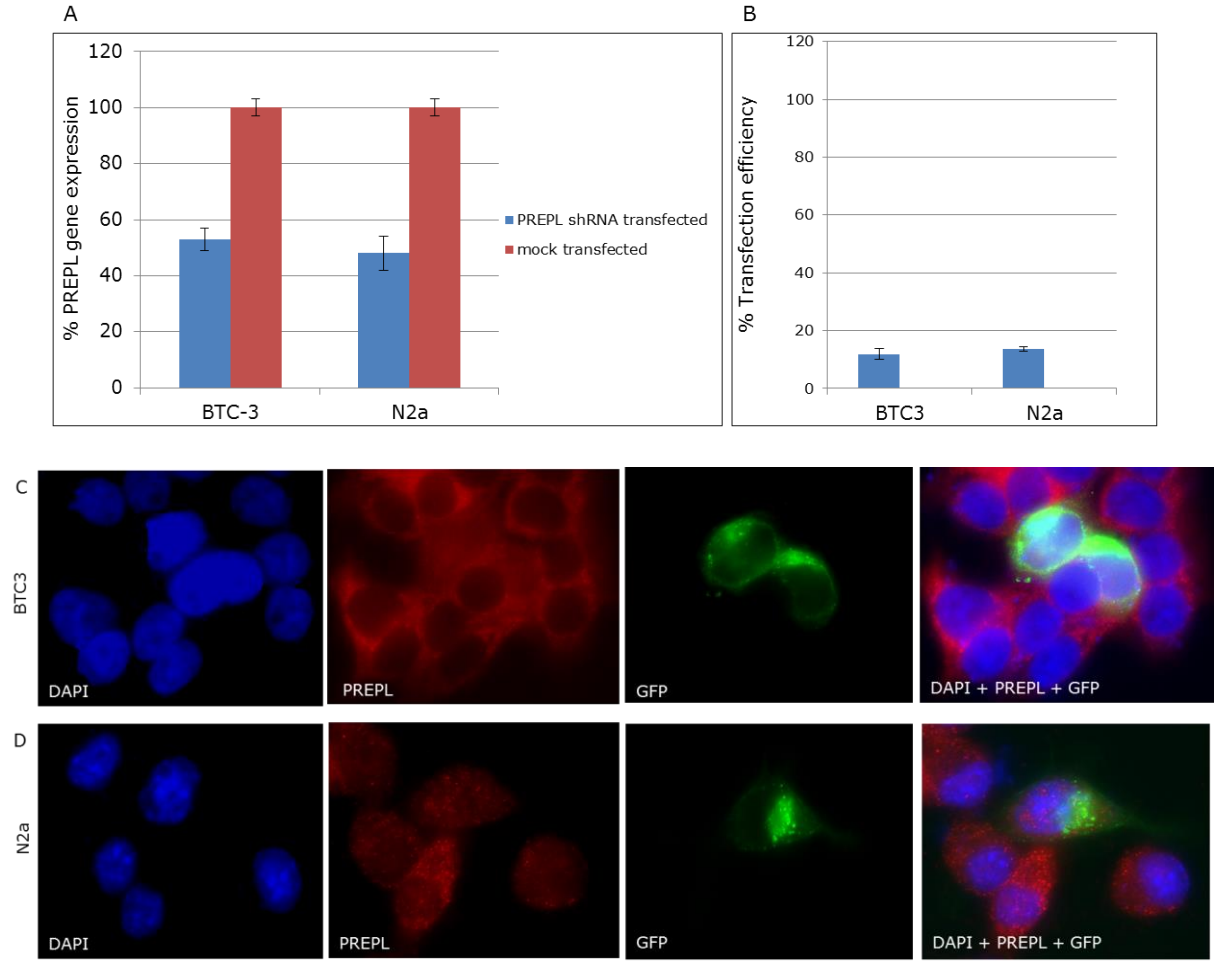


Figure 8. shRNA efficiency in silencing PREPL gene expression in βTC-3 and N2a cells. A: Comparing PREPL gene expression between shRNA transfected and mock transfected by qPCR, shRNA was able to silence 48% and 52% of PREPL gene expression in βTC-3 and N2a respectively. B: βTC-3 cells and N2a cotransfected with shRNA and phogin-GFP showed only 13% and 14% from 100 cells, respectively, were phogin-GFP positive. C-D: immunostaining of βTC-3 cells (C) and N2a cells (D). Blue is Dapi staining, red is PREPL staining, green is phogin-GFP.

### *3.2.3 Phogrin-pHluorin transfection efficiency*

To determine the effect of PREPL deficiency in vesicles secretion and fusion with the plasma membrane by live cell imaging, we used a phogrin-pHluorin construct (a generous gift by Dr. Ohara-Imaizumi, Kyorin University School of Medicine, Tokyo, Japan).

As a transmembrane protein, phogrin is localised within insulin-containing vesicles, with its C-terminus located in the cytosol and N-terminus in the lumen [35]. During maturation of secretory vesicles, the dibasic residues ($Lys^{414}$ and $Lys^{416}$) of phogrin in lumen has to be cleaved. In this construct, the dibasic residues were mutated into $Asn^{414}$ and $Asn^{416}$ to prevent cleavage. The N-terminus of ecliptic pHluorin, a pH-sensitive GFP variant activated around pH 7.4, was inserted next to the signal peptide of truncated phogrin construct (Figure 9). In this way, a tandem phogrin-pHluorin construct is generated that remains attached during endocytosis and exocytosis. This construct is cloned into pCI-Neo mammalian expression vector. As pHluorin is located inside the lumen of vesicles with acidic pH (<5.5), it is only visible when the vesicles are fused with plasma membrane, exposing the content into the cytosol with pH of 7.4, causing pHluorin to emit its fluorescence [36].

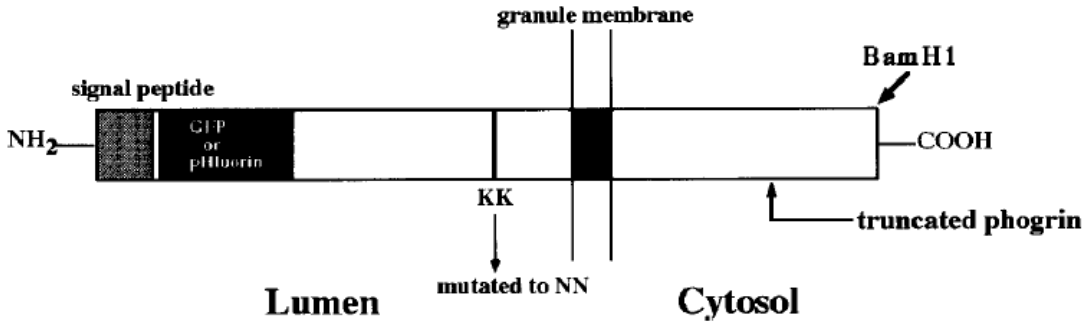


Figure 9. Phogrin-pHluorin construct. N-terminus of phogrin is located in the lumen, while C-terminus is located in the cytosol. N-terminus of pHluorin is attached to the signal peptide of phogrin which cleavage sites have been mutated from $Lys^{414}$ and $Lys^{416}$ (KK) into $Asn^{414}$ and $Asn^{416}$ (NN). This region was then attached to the truncated phogrin and the construct was digested by BamH1 [36].

Expression of phogrin-pHluorin was confirmed by transfecting βTC-3 with the contruct. Transfection with phogrin-GFP was done in paralel as a transfection control. Phogrin expression was detected by rabbit polyclonal anti-phogrin developed by the lab of Prof. Creemers, and observed by both western blot and immunostaining. The immunofluorescence showed high signal intensity for phogrin (Figure 10a). As pHluorin is invisible unless it comes into contact with extracellular environment and emits its fluorescence, it was not possible to check the presence of pHluorin by immunostaining.

The molecular weight of phogrin is reported to be approximately 64 kDa [37], and both GFP and pHluorin have weight of 27 kDa [38]. The signals detected by western blot showed bands at approximately 90 kDa, which confirmed the presence of phogrin-pHluorin and phogrin-GFP in the cells (Figure 10b).

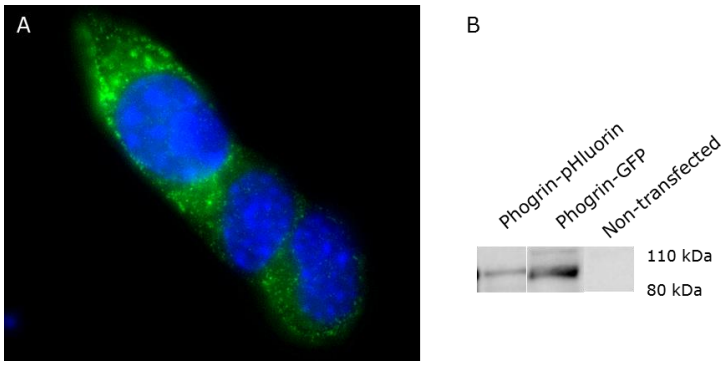


Figure 10. Phogrin expression in phogrin-pHluorin construct. A: βTC-3 cells transfected with phogrin-pHluorin construct. B: βTC-3 transfected with either phogrin-pHluorin or phogrin-GFP, or non-transfected. Both constructs were detected at approximately 90kDa in both cells.

Optimising co-transfection of βTC-3 cells with shRNA, phogrin-pHluorin, and internal fluorescent marker with different fluorescent colour than green are still warranted to eventually monitor the dynamic of secretory vesicles by live cell imaging. In this procedure, the distribution and time course of basal and stimulated LDCVs secretion in single cells before and after PREPL knockdown will be evaluated. This procedure will still be performed in the near future.

### 3.5 AP-1 and TGN colocalisation in Mouse Embryonic Fibroblast cells

Previously, Radhakrishnan K, et al. [31] reported that PREPL influenced AP-1 redistribution. The study was performed in fibroblast of HCS patients and human control, as well as in HeLa cells with PREPL knockdown by RNAi. As AP-1 is usally used as a TGN marker, the cells were treated with anti-AP-1, and the effect of PREPL deficiency in AP-1 dispersal was observed by confocal microscopy. The results indicated that absence of PREPL in patients fibroblast led to more intense staining and bigger TGN area, while PREPL deficiency in HeLa cells gave a more intense staining of TGN but with less pronounced distribution than in patients fibroblast. In addition, overexpressing PREPL in MEF cells decreases TGN binding AP-1.

In the present study, we tried to confirm AP-1 redistribution in PREPL deficiency cells by conducting double immunostaining with AP-1 and TGN46 antibody to PREPL KO MEFs and wild-type. The application of double immunostaining will provide more appropriate analysis of AP-1 co-localisation in the TGN. Moreover, the availability of cells from PREPL knockout mice is an easier and more straightforward approach rather than downregulating PREPL expression by RNAi.

Our immunostaining results showed that, the localisation of AP-1 was spread out in the cytosol and slightly denser in the TGN area in MEF WT (Figure 11 top). In most PREPL KO MEF cells, AP-1 was shown to be clustered at the TGN with brighter staining than in MEF wild-type. This indicated that there were more co-localisation between AP-1 and TGN observed in PREPL KO MEFs shown by the overlapping fluorescent green and red in comparison to MEF wild-type. Furthermore, there was less AP-1 in the cytosol of PREPL KO MEFs compared to wild-type MEFs (Figure 11 bottom). Even though our current results were not quantified, they confirmed that PREPL deficiency leads to accumulation of AP-1 in TGN [31]. Nevertheless, it will be of additional value to quantify AP-1 signal intensity in the TGN in the future. Our results hence confirmed the results by Radhakrishnan

K, et al in HeLa cells with PREPL knockdown, in which AP-1 displayed a more intense staining at the TGN. In our first attempt co-localisation in patient's fibroblast unfortunately failed since our TGN antibody did not have affinity towards human cells. In the future different TGN markers will be tested to confirm the results in human patient fibroblasts.

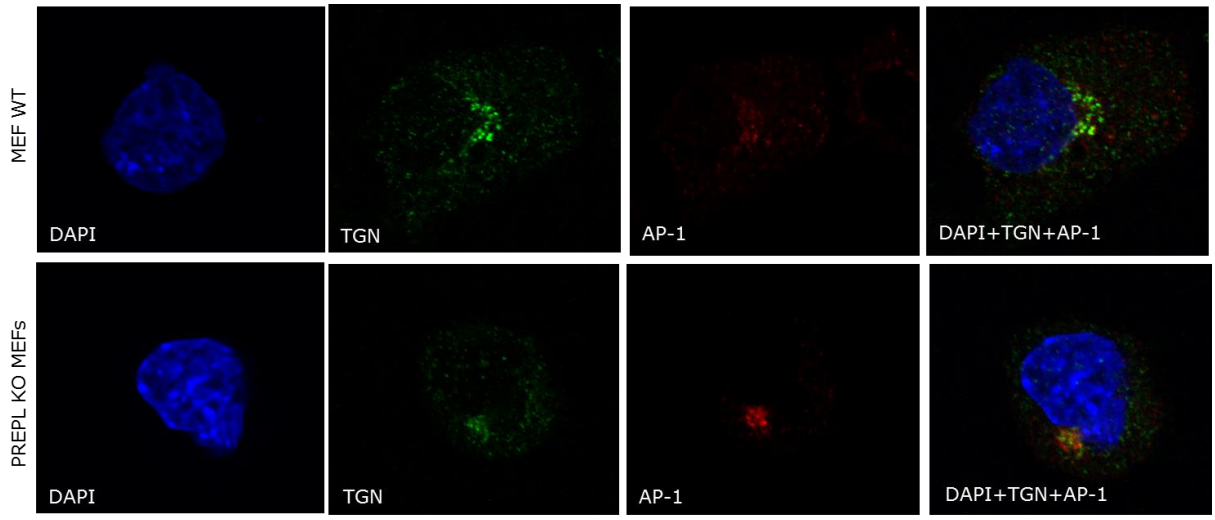


Figure 11. AP-1 and TGN colocalisation in PREPL KO MEFs and wild-type MEFs as observed by confocal microscopy. Top: Wild-type MEF cells. Bottom: PREPL KO MEFs . Blue Dapi staining represents nucleus, green represents TGN, and red represents AP1.

It is already known that the function of AP-1 in exocytosis requires Arf-GTP, phosphatidylinositol 4-phosphate (PI-4-P), and a cargo protein containing the AP-1 binding motif. The process of vesicles formation is initiated by exchanging GDP to GTP in Arf which is performed by guanine nucleotide exchange factor (GEF). This binding of GTP leads to activation of Arf [39] that will recruit inactive AP-1 from the cytosol to the vesicle membrane via binding the γ1 and β1 subunit. This AP-1 activation will in turn sorts cargo protein, recruits effector proteins involved in vesicles formation, and initiate clathrin recruitment to start forming into lattice shape [40], [31]. Once cargo is sorted and the vesicle coat is formed, the coat membrane polarizes and buds from the non-coated membrane. This event involves a regulator protein known as Arf GTPase-activating protein (GAP) that hydrolyses GTP to GDP, hence converting Arf back to its inactive form (Arf-GDP) [41].

The fact that PREPL deficiency leads to AP-1 localisation at the TGN indicates that Arf1-GTP was able to recruit AP-1 from cytosol to TGN to assemble clathrin-coated vesicles. However, the lack of AP-1 in the cytosol suggests that vesicles' budding from the TGN is interrupted. A plethora of processes occur in order to have proper vesicles release and this involves many protein-protein interactions. Therefore, several causes can drive the defect in vesicles budding. One possibility is that the Arf-GTP remains active perhaps due to decreased activity of GAP or increased activity of GEF. As long as Arf-GTP is active, AP-1 and clathrin will be recruited to the TGN. Vesicles formation is thus hindered, creating a sustain binding of AP-1 in TGN and can explain unilocal distribution of AP-1 to the TGN [41], [42].

The exact mechanism on how PREPL affects AP-1 localisation and vesicle budding is hard to determine. Nevertheless, the data to date show that PREPL is involved in vesicle regulation and its absence disrupts vesicles transport from the TGN. As our previous findings showed that PREPL deficiency leads to decreased vesicles secretion in βTC-3 cells which has regulated secretion, it will be essential to confirm PREPL and AP-1 co-localisation as well as the effect of PREPL deficiency in AP-1 distribution in TGN in βTC-3 cells. This correlation will serve as solid basis for further studies elucidating the exact function of PREPL in AP-1 mediated protein export.

### 3.6 Patients study, novel deletion characterisation

In this genetic study, we conducted deletion screening to determine breakpoints on 8 candidate HCS patients from The Netherlands, Belgium, and Italy. In 4 of these patients, array-Comparative Genomic Hybridization (array-CGH) was performed previously by Laboratory of Clinical Genetics. Array-CGH is a technique in which genomic DNA samples are hybridized to reference DNA in order to determine copy number variations and chromosomal aberrations[43]. The array-CGH results revealed breakpoints that included deletion of PREPL, SLC3A1, and/or C2Orf34. Here, we aimed to confirm the known deletion, as well as characterising novel deletion. The latter includes determining the number of deleted alleles of different exons in SLC3A1, PREPL, and C2Orf34, and narrow down the borders of these new deletion by quantitative PCR.

#### *3.6.1 Patient 1, 2, 3, and 4*

Patients 1 and 2 are both Belgians and the patient samples were retrieved from Dr. Legius from the Hospital of Leuven University (Leuven, Belgium) and Dr. De Rouck from the Hospital of Sint Josef (Turnhout, Belgium), respectively. While patient 1 exhibits mental retardation, epilepsy, and hypotonia, patient 2 exhibits poor facial mimicry and psychomotor retardation which is characterised by slow speech, poor facial expression, and impaired gross motor skills [44]. The array-CGH results from both patients showed the boundaries of deletion started at SLC3A1 intron 1 and ended in PREPL intron 1.

We conducted qPCR using patients genomic DNA to confirm the results from array-CGH. Both patients have heterozygous deletion from SLC3A1 exon 2 to PREPL exon 2 (Figure 12a and b), while SLC3A1 exon 1 and PREPL exon1 are still present on both alleles. This suggests that breakpoints are located in SLC3A1 intron 1 and PREPL intron 1. Since this deletion shared the same pattern with deletion B (75.5 kb) in HCS (Figure 2), junction fragment PCR specific for this deletion was performed to confirm it. Two additional patients from the Netherlands were included. The samples were retrieved from Dr. Régal from the Hospital of Leuven University. The patients were brothers and both exhibit classical HCS features with neonatal hypotonia, neonatal feeding problems, adult obesity and persistent ptosis and facial weakness. Neither array-CGH nor qPCR had been performed prior junction fragment PCR for these 2 brothers. Genomic DNA from a patient with definite HCS deletion B was used as a positive control and a healthy control was used as a negative control. If positive, the junction fragment PCR results in a 1.2 kb amplicon that is absent in healty individuals (Figure 12b). The results confirmed that all 4 patients had in fact deletion B, with patient 1 and 2 as carriers (Figure 12c).

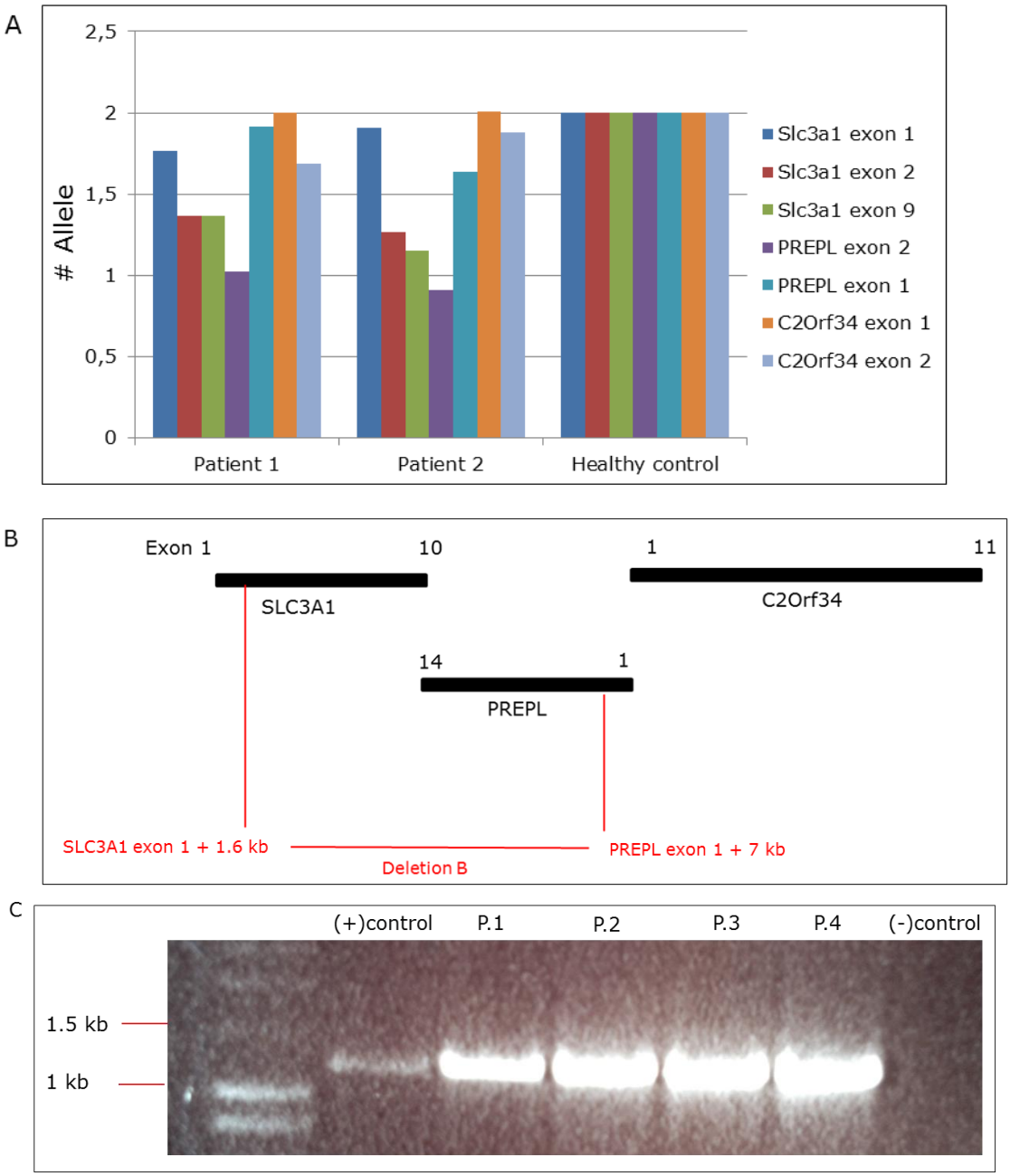


Figure 12 (A). Overview of deletion screening in patient 1 and 2 by qPCR. This screening shows heterozygous deletion from SLC3A1 exon 2 until PREPL exon 2, while SLC3A1 exon 1 and PREPL exon1 are still present. (B) approximate position of annealing primers for deletion B in patient 1 and 2. (C) Junction fragment PCR for deletion B; positive control, P.1: patient 1, P.2: patient 2, P.3: patient 3, P.4: Patient 4, negative control.

### *3.6.2 Patient 5*

Samples from patient 5 were obtained by Dr. De Ravel from the Hospital of Leuven University. The patient exhibits mental retardation and self aggression, and the array-CGH results suggest that breakpoints are located in PREPL intron 5 and 7. Quantitative PCR showed the presence of both alleles for PREPL exon 5 and 8, and only presence of single allele for PREPL exon 6 and 7 (Figure 13a and b). For this patient, primers are currently being designed and tested for junction fragment PCR. Sequencing of the amplicon of the junction fragment PCR will allow determination of the exact breakpoints in this patient.

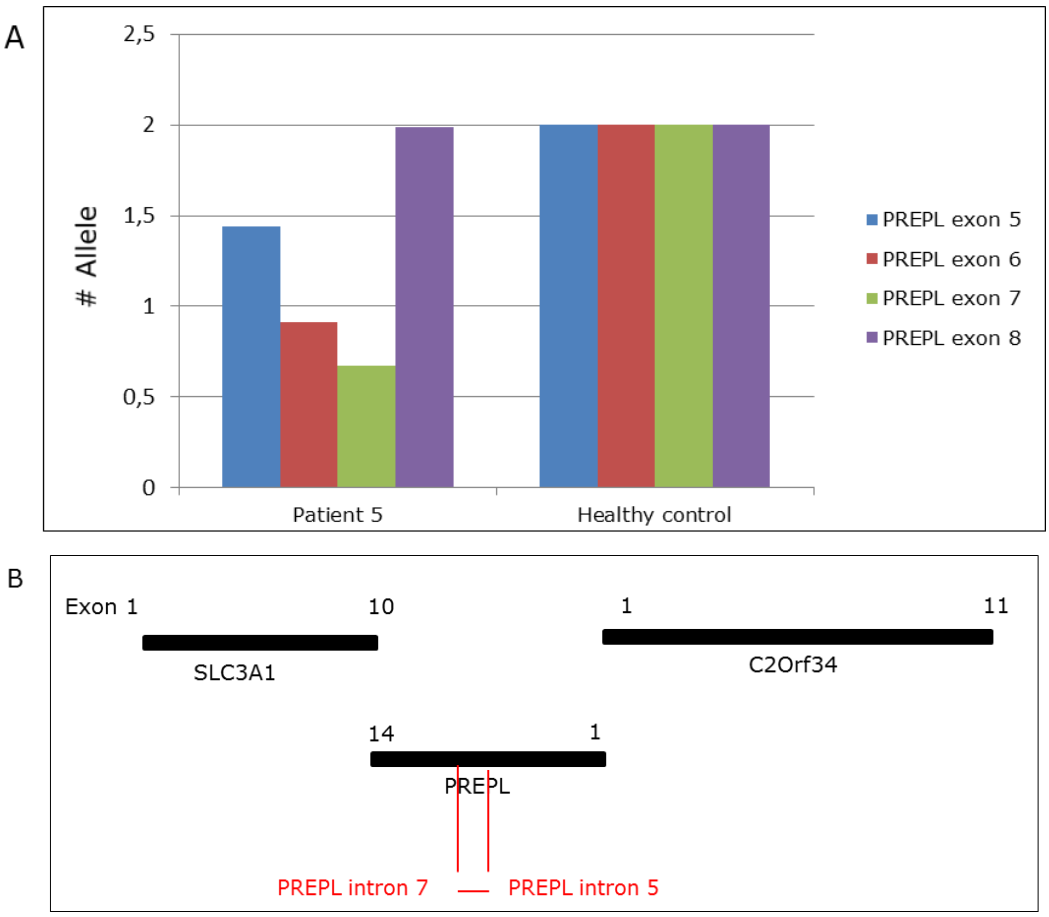


Figure 13 (A). Deletion screening of patient 5, showing heterozygous deletion of PREPL exon 6 and 7. (B) Breakpoint position in patient 5.

### *3.6.3 Patient 6*

Patient 6 was recruited by Dr. Van Esch from Hospital of Leuven University. Obesity, intelectual disability, dysmorphism, amblyopia and self aggression are the observed clinical features, and array-CGH identified deletion in exon 12 of PREPL up to intron 2 of C2Orf34. Deletion screening by qPCR confirmed the presence of PREPL exon 13 and C2Orf34 exon3 (Figure 14a). The results confirmed a heterozygous deletion spanning from PREPL exon 12 up to C2Orf34 exon 2 (Figure 14a and b). Similar to patient 5, junction fragment PCR and sequencing are also currently being designed and tested to determine the exact breakpoints.

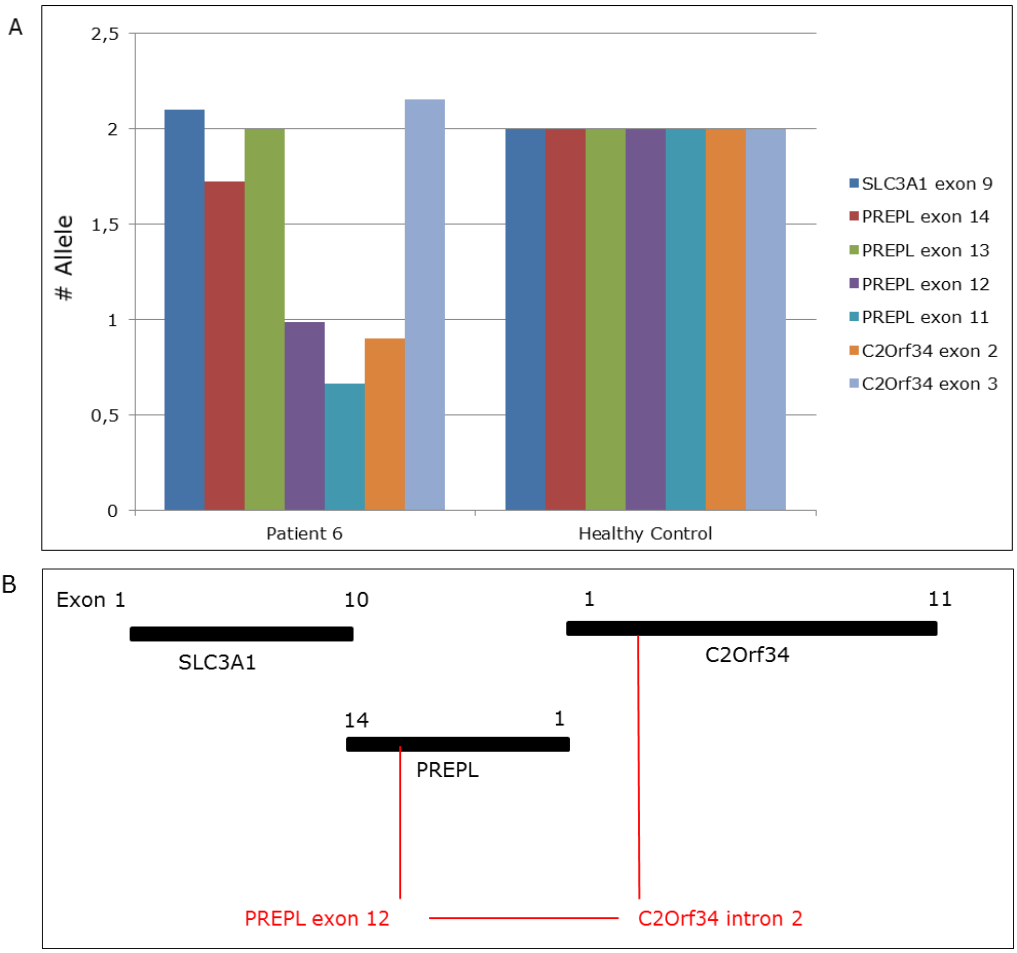


Figure 14 (A). Deletion screening of patient 6 by quantitative PCR revealing deletion that spans from PREPL exon 12 to C2Orf34 exon 2. (B) Position of deleted sequence in patient 6.

### *3.6.4 Patient 7 and 8*

Patients 7 and 8, a son and his mother, were clinically suggested by Dr. Burlina from the Hospital of Padova (Padova, Italy) to perform deletion screening on their genomic DNA by the lab of Prof. Creemers. The son displayed neonatal hypotonia, feeding problems and cystinuria. SLC3A1, PREPL and C2Orf34 loci screened by qPCR for the son and the parents indicating that the proband was heterozygous for maternal deletion involving SLC3A1, PREPL, and C2Orf34 (Figure 15b). In both patients, SLC3A1 intron 6 until C2Orf34 exon 2 was missing in one allele, while both alleles for SLC3A1 exon 6 were still present. C2Orf34 exon 3 had been screened previously and showed the presence of this exon in both alleles in both patients.

For determining the approximate locations of breakpoints, new qPCR primers were designed. The beginning of the breakpoint is located in SLC3A1 intron 6. The distance between reverse primer of exon 6 (GGAATGCACGA) and forward primer of intron 6 is approximately 1500 bp (GGAATGCACGA+1500bp). To obtain closer proximity to the beginning of breakpoint, a new primer set was designed using Probe Finder (Roche). The primers are located approximately 600bp downstream of exon 6 (GGAATGCACGA+600bp, addressed as SLC3A1 intron 6 (600bp)), with an amplicon size of 61 nucleotides (Red box figure 15a). Screening of this new amplicon revealed that

this fragment was absent in 1 allele for both patients (Figure 15b). Therefore, the proximal boundary of deletion in patient 7 and 8 is determined to be SLC3A1 intron 6 (600bp).

The distal boundary of breakpoint is located within intron 2 of C2Orf34 which has size a of 17000 bp. Twelve primer sets (supplementary data 1) were designed with an approximately 1000 bp distance from each other and each primer sets generate maximum 100 bp amplicons (Figure 15a). At 3000 bp downstream of intron 2, qPCR reported that this sequence is missing. Further assessment with different sets of primer is still needed to be performed to determine the exact end of breakpoints in the genome. By identifying these breakpoints, junction fragment PCR can be performed to confirm the deletion, followed by sequencing of this junction fragment to determine the exact location of breakpoints.

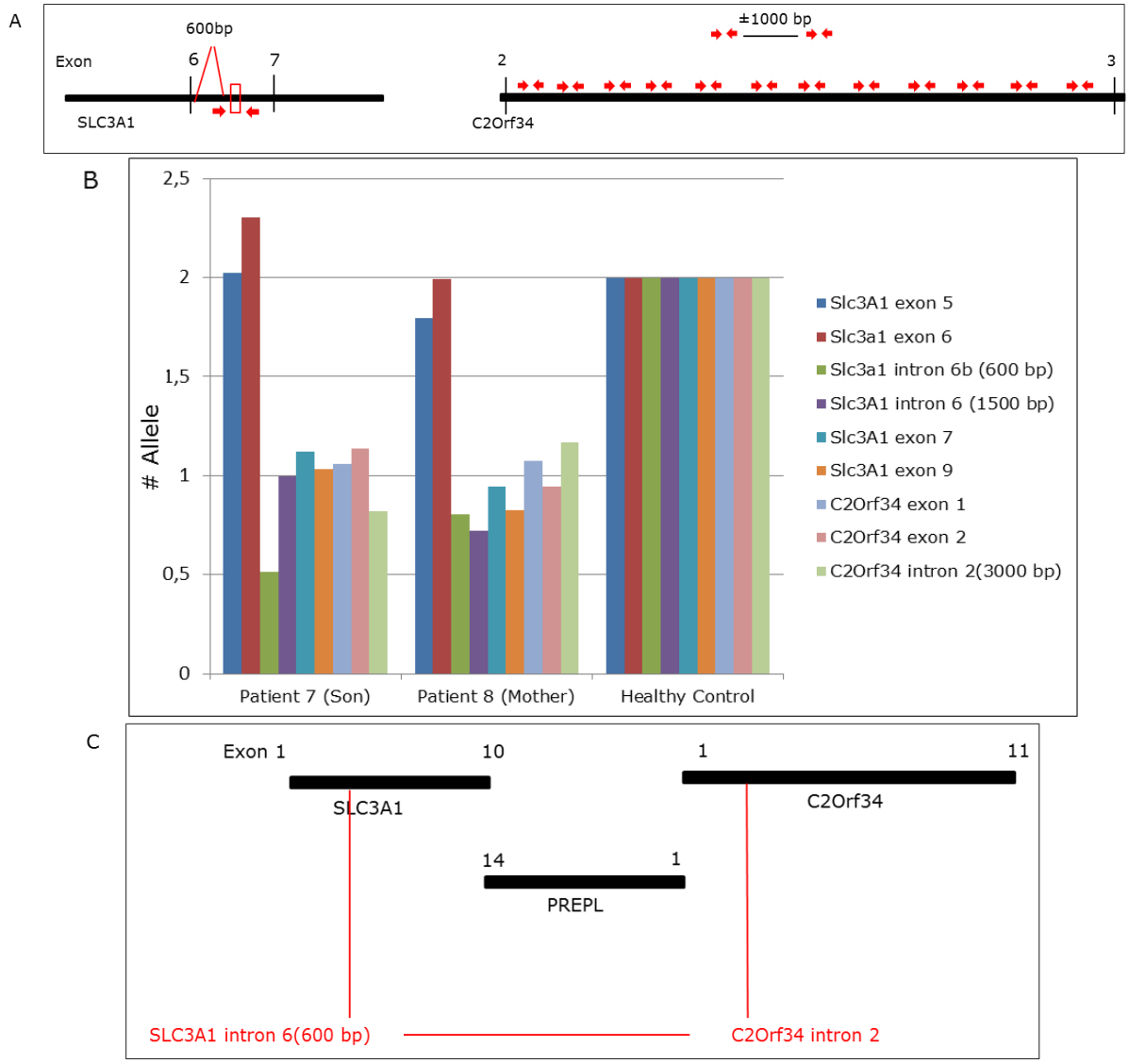


Figure 14 (A). Scheme of a new primer set for breakpoints in SLC3A1 intron 6 and 12 primers sets for C2Orf34 intron 2. Figure 14 (B and C). Overview of breakpoint screening from patient 7 and 8 by qPCR

HCS has been described in 17 families and it is globally distributed. In this study, we were able to describe 4 patients from Netherlands and Belgium with deletion B, one of the most frequent HCS deletions. Two of them (patient 1 and 2) appear to be carriers of this deletion. Despite the results

from quantitative PCR that showed deletion of SLC3A1 downstream of intron 1 for patient 1 and 2, cystinuria type I was not reported. As Cystinuria type I is a recessive trait, heterozygous deletion of SLC3A1 might give normal profile of cystine excretion in the urine [45].

It was observed that mental retardation, hypotonia, obesity, or dysmorphism shown by the patients are accompanied by the loss of PREPL, either homozygous or heterozygous. Several clinical studies in 2p21 deletion syndrome and HCS reported that as the absence of SLC3A1 causes isolated cystinuria type 1, the other characteristics such as hypotonia are likely to be attributed to deletion of PREPL functionality [13], [9]. This premise is supported by a recent study of a patient with isolated PREPL deficiency who develops myasthenic syndrome, a neuromuscular disorder characterised by muscle weakness [46]. The patient shows neonatal hypotonia, feeding difficulties, ptosis, low insulin-like growth factor 1, growth hormone deficiency, and no cystinuria was developed. Genetic proband analysis revealed maternal deletion of PREPL and SLC3A1 and paternal PREPL nonsense mutation. Since cystinuria was not observed in proband, her myasthenic profile is determined by the absence of PREPL. Immunostaining results showed the absence of PREPL in muscle fiber and endplates of this patient, verifying that the myasthenic symptoms shown in HCS is due to homozygous PREPL deletion [14].

Some patients in this study exhibit hypotonia even though their PREPL gene is absent only in 1 allele. This is interesting because as a recessive trait, carriers of HCS are asymptomatic. In addition, Patient 5 in this study reveals heterozygous deletion involving PREPL exon 6 and 7 but myasthenic symptoms are not observed. This observation suggests that hypotonia shown by HCS carriers might also due to several factors other than loss of PREPL, such as other genetic defect, GTP cyclohydrolase I deficiency and chromosome 22 deletion [47], [48]. Deletion from PREPL exon 12 to C2Orf32 intron 2 (Patient 6), deletion of PREPL exon 6 and 7 (Patient 5), and deletion SLC3A1 intron 6 to C2Orf34 intron 2 (Patient 7 and 8) have not been described in the literature. Therefore, these deletions appear to be novel.

Besides serving as a methyltransferase, little is known about the function of C2Orf34. The deleted C2Orf34 in 2p21 deletion syndrome and atypical HCS, however, gives additional symptoms with mild to moderate mental retardation [13]. Parvari et al [49] showed in their study that deletion of the beginning of C2Orf34 in 2p21 deletion syndrome led to increased amount of hypomethylated Calmodulin. Calmodulin mediates Calmodulin-dependent signaling which is also important for proper neuronal development [50]. Therefore, the lack of methylated calmodulin due to loss of C2Orf34 may results in mental retardation in 2p21 deletion syndrome and atypical HCS.

Nevertheless, mental retardation has been recently observed in patients with PREPL and SLC3A1 deletion alone (Patient 1 and 2), or patients with deletion in PREPL alone (patient 5). Several additional symptoms from the patients reported here such as self aggression (Patient 5 and 6) and amblyopia (patient 6) have not been reported in HCS case. A study by Rauch A, et al also mentioned several features in patients with deleted PREPL and C2Orf34 that are not displayed in 2p21 deletion syndrome and atypical HCS such as genital anomaly (hypoplastic labia majora) and bossing forehead [11]. Another patient described by Zaffanello, et al showed an interesting genetic

analysis. Despite the molecular analysis revealed homozygous deletion B, the patient exhibited all HCS symptoms with the addition of mitochondrial respiratory defect, which has not been reported in other HCS case [51].

The complexity and severity of phenotypes are indeed depend on a number of factors such as number of genes involve, the size of deletion, homozygosity and heterozygosity but also ethnicity plays an important role. Nonetheless, it is possible that there are gene-gene interactions outside the deleted regions, modifier genes, genes defect, or even environmental influences that have yet to be discovered, that might influence the profile of the patients.

# 4. Conclusion and Future Perspective

Hypotonia Cystinuria Syndrome (HCS) is a congenital recessive disease characterised by cystinuria type I, neonatal hypotonia, growth hormone deficiency and feeding problem. It is caused by deletion of *SLC3A1* and *PREPL* which are adjacently located in chromosome 2p21. There are 17 familes globally distributed with 9 different HCS deletions that have been reported to date. Loss of SLC3A1 causes cystinuria type I, and homozygous PREPL deletion leads to myasthenic syndrome in HCS. Substrates and molecular functions of PREPL are not known yet. However, the fact that PREPL deficiency decreases regulated secretion of LDCVs, and PREPL acts as an effector of AP-1 which mediates vesicles secretion lead to our hypothesis in which PREPL is involved in regulated secretion. In the present study, we tried to characterise the pathophysiology of PREPL deficiency by means of immunocytochemical and genetics studies.

Two commercial PREPL antibodies for immunostaining and western blot were optimised in HEK293T, βTC-3, and wild-type MEFs and PREPL KO MEFs to check the specificity. In immunostaining, the mouse anti-PREPL (B01) antibody works against mouse and human cells at concentration of 1/100 while the mouse anti-PREPL (E9) antibody works against human cells at concentration of 1/50. In western blot, PREPL expression in HEK293T, βTC-3, and wild-type MEFs was hardly detected by the B01 antibody, unless human PREPL was overexpressed in HEK293T. Meanwhile, the E9 antibody was able to detect endogenous PREPL and human PREPL overexpressed in HEK293T via Western blot, but unable to visualise that in βTC-3 and MEF wild-type.

In order to study the influence of PREPL deficiency in vesicles secretion and fusion to plasma membrane by live cell imaging, we developed shRNA to knockdown PREPL expression in mouse cells. In murine cell lines the shRNA efficiency in knocking down PREPL gene in βTC-3 was approximately 48%, while the transfection efficiency was only 13% as judged by the amount of GFP-positive colonies by immunofluorescence. This disrepancy might be influenced by different amount of cells and amount of transfected constructs in both approaches. In the future, utilizing the same amount of cells as well as transfection with single construct is considerable. The transfection efficiency and shRNA knockdown efficiency will be evaluated by FACS. Important to note is that it would be of course an option to check shRNA efficiency in knocking down protein expression using Western blot analysis. Unfortunately, there are currently no suitable antibodies available and they need to be developed to address this issue more appropriately in the future. Finally, it might also be better in the future, to replace transient shRNA expression using the plasmid vector strategy used in described research with stable integration using a viral vector system as the later will produce a stable cell line with PREPL knockdown.

Phogrin expression in phogrin-pHluorin construct for live cell imaging was checked by western blot and immunofluorescence. As pHluorin is located in the lumen and only emits fluorescence when it comes into contact with plasma membrane, immunofluorescence was not an option to show its expression. However, as phogrin has mass of approximately 64 kDa, and phluorin has mass of 27

kDa, the presence of signals at approximately 90 kDa in western blot suggested that phluorin was as well expressed. In the near future, live cell imaging can be done by co-transfecting βTC-3 cells with shRNA, phogrin-pHluorin construct, and an immunofluorescent internal control.

We also confirmed the effect of PREPL deficiency in AP-1 and TGN co-localisation by using MEF cells with PREPL knockout and MEF wild type. While in MEF wild type, AP-1 is shown to be dispersed in the cytosol, PREPL knock out in MEF led to accumulated AP-1 in the TGN area. It is possible that PREPL deficiency affects the Arf GTP to remain active, and thus continuously recruiting AP-1 to TGN. The failure in forming vesicles properly may affect AP-1 binding on TGN. In order to verify the theory that PREPL is involved in regulated secretion, co-localisation of AP-1 and PREPL as well as AP-1 and TGN in cells with regulated secretion such as βTC-3 cells need to be validated.

It will be interesting as well to perform yeast-2-hybrid by using PREPL as a bait. As little is known about molecular function, substrates, and interacting partners of PREPL, yeast-2-hybrid might give an overview of genes that interact with PREPL. The resulting interaction partners will be linked with the potential function of PREPL and may provide a mechanistic explanation.

Deletion screening by quantitative PCR was done to 8 patients from Netherlands, Belgium, and Italy. Four patients were reported to have deletion B that spans from SLC3A1 intron 1 to PREPL intron 1, in which 2 of them are carriers. This also confirmed the high prevalence of previously reported deletion B HCS in northern Europe. One Belgian patient has heterozygous deletion from PREPL intron 5 to intron 7, and another Belgian patient has heterozygous deletion from PREPL exon 12 to C2Orf34 intron 2. An italian family (son and mother) have heterozygous deletion for SLC3A1 until C2Orf34. The proximal breakpoints starts in intron 6, 600 bp downstream of exon 6. The distal breakpoint is located in C2Orf34 intron 2, however the exact location has yet to be determined. For patients which deletions have not been determined yet, junction fragment PCR and sequencing are substantial to confirm the deletion and establish the exact breakpoints, respectively. Knowing the exact breakpoints allows for using junction fragment PCR in the future as a diagnostic tool in certain populations, and informs us whether the deletion is novel or not.

Our findings support the knowledge so far, indicating that PREPL is involved in vesicles secretion by interracting with AP-1. To confirm our hypothesis, however, more research is warranted. Elucidating the role of PREPL in regulated secretion will form the backbone for further research, such as the molecular mechanism behind its function. Together with better diagnostic tools, it will be possible to improve the treatment of HCS patients to ease the hypotonia.

# 5. Reference List


1. Schwartz, S. and M.D. Graf, *Microdeletion syndromes. Characteristics and diagnosis.* Methods Mol Biol, 2002. **204**: p. 275-90.
2. Clara, R. and A. Lowenthal, *[Familial aminoaciduria with muscular hypotonia and dwarfism].* Bull Acad R Med Belg, 1966. **6**(9): p. 577-611.
3. Eggermann, T., et al., *2p21 Deletions in hypotonia-cystinuria syndrome.* Eur J Med Genet, 2012. **55**(10): p. 561-3.
4. Regal, L., et al., *Two novel deletions in hypotonia-cystinuria syndrome.* Mol Genet Metab, 2012. **107**(3): p. 614-6.
5. Martens, K., *Characterisation of PREPL, a putative serine oligopeptidase deleted in patients with hypotonia-cystinuria syndrome*. 2006, KU Leuven.
6. *Prader-Willi Syndrome: Introduction*. Available from: http://library.thinkquest.org/06aug/00440/mpraderintro.html.
7. Kilic, E., G.E. Utine, and K. Boduroglu, *A case of Sotos syndrome with 5q35 microdeletion and novel clinical findings.* Turk J Pediatr, 2013. **55**(2): p. 207-9.
8. McMullan, T.F., et al., *A novel X-linked dominant condition: X-linked congenital isolated ptosis.* Am J Hum Genet, 2000. **66**(4): p. 1455-60.
9. Jaeken, J., et al., *Deletion of PREPL, a gene encoding a putative serine oligopeptidase, in patients with hypotonia-cystinuria syndrome.* Am J Hum Genet, 2006. **78**(1): p. 38-51.
10. *SLC3A1*. 2014.
11. Bartholdi, D., et al., *Further delineation of genotype-phenotype correlation in homozygous 2p21 deletion syndromes: first description of patients without cystinuria.* Am J Med Genet A, 2013. **161A**(8): p. 1853-9.
12. Wei, J. and B.S. Liang, *PPM1B and P-IKKbeta expression levels correlated inversely with rat gastrocnemius atrophy after denervation.* Braz J Med Biol Res, 2012. **45**(8): p. 711-5.
13. Chabrol, B., et al., *Deletion of C2orf34, PREPL and SLC3A1 causes atypical hypotonia-cystinuria syndrome.* J Med Genet, 2008. **45**(5): p. 314-8.
14. Regal, L., et al., *PREPL deficiency with or without cystinuria causes a novel myasthenic syndrome.* Neurology, 2014. **82**(14): p. 1254-60.
15. Martens, K., et al., *PREPL: a putative novel oligopeptidase propelled into the limelight.* Biol Chem, 2006. **387**(7): p. 879-83.
16. Parvari, R., et al., *The 2p21 deletion syndrome: characterization of the transcription content.* Genomics, 2005. **86**(2): p. 195-211.
17. Morawski, M., et al., *Cellular and ultra structural evidence for cytoskeletal localization of prolyl endopeptidase-like protein in neurons.* Neuroscience, 2013. **242**: p. 128-39.
18. GM, C., *Endocytosis*. 2nd ed. The Cell: A Molecular Approach

2000, Sunderland: Sinauer Associates.

19. Cooper, G., *The Cell: A molecular approach*. 2 ed. 2000, New York: Garland Science.
20. Alberts B, e.a., *Essential Cell Biology: Intracellular compartment and transport*. 3 ed. 2009, New York: Garland Science.
21. Alberts B, e.a., *Molecular Biology of the Cell*. 5 ed. 2008, New York, USA: Garland Science.
22. Scalettar, B.A., *How neurosecretory vesicles release their cargo.* Neuroscientist, 2006. **12**(2): p. 164-76.
23. Vardjan, N., J. Jorgacevski, and R. Zorec, *Fusion pores, SNAREs, and exocytosis.* Neuroscientist, 2013. **19**(2): p. 160-74.
24. Harata, N.C., A.M. Aravanis, and R.W. Tsien, *Kiss-and-run and full-collapse fusion as modes of exo-endocytosis in neurosecretion.* J Neurochem, 2006. **97**(6): p. 1546-70.

25. Tissot, J.D., *Blood microvesicles: From proteomics to physiology.* Translational Proteomics, 2013. **1**(1): p. 38-52.
26. Schmid, S.L., *Clathrin-coated vesicle formation and protein sorting: an integrated process.* Annu Rev Biochem, 1997. **66**: p. 511-48.
27. Robinson, M.S. and J.S. Bonifacino, *Adaptor-related proteins.* Curr Opin Cell Biol, 2001. **13**(4): p. 444-53.
28. Bonnemaison, M.L., B.A. Eipper, and R.E. Mains, *Role of adaptor proteins in secretory granule biogenesis and maturation.* Front Endocrinol (Lausanne), 2013. **4**: p. 101.
29. Rodriguez-Boulan, E., G. Kreitzer, and A. Musch, *Organization of vesicular trafficking in epithelia.* Nat Rev Mol Cell Biol, 2005. **6**(3): p. 233-47.
30. Burgos, P.V., et al., *Sorting of the Alzheimer's disease amyloid precursor protein mediated by the AP-4 complex.* Dev Cell, 2010. **18**(3): p. 425-36.
31. Radhakrishnan, K., et al., *Trans-Golgi network morphology and sorting is regulated by prolyl-oligopeptidase-like protein PREPL and the AP-1 complex subunit mu1A.* J Cell Sci, 2013. **126**(Pt 5): p. 1155-63.
32. Royle, S.J., et al., *Imaging phluorin-based probes at hippocampal synapses.* Methods Mol Biol, 2008. **457**: p. 293-303.
33. Microbe Inotech Laboratories, I. *Quantitative Real-Time PCR (qPCR)*. Available from: http://www.microbeinotech.com/Default.aspx?tabid=177.
34. Rao, D.D., et al., *siRNA vs. shRNA: similarities and differences.* Adv Drug Deliv Rev, 2009. **61**(9): p. 746-59.
35. Caromile, L.A., et al., *The neurosecretory vesicle protein phogrin functions as a phosphatidylinositol phosphatase to regulate insulin secretion.* J Biol Chem, 2010. **285**(14): p. 10487-96.
36. Ohara-Imaizumi, M., et al., *Monitoring of exocytosis and endocytosis of insulin secretory granules in the pancreatic beta-cell line MIN6 using pH-sensitive green fluorescent protein (pHluorin) and confocal laser microscopy.* Biochem J, 2002. **363**(Pt 1): p. 73-80.
37. Wasmeier, C. and J.C. Hutton, *Secretagogue-dependent phosphorylation of the insulin granule membrane protein phogrin is mediated by cAMP-dependent protein kinase.* J Biol Chem, 2001. **276**(34): p. 31919-28.
38. Schulte, A., et al., *A novel fluorescent pH probe for expression in plants.* Plant Methods, 2006. **2**: p. 7.
39. Cohen, L.A. and J.G. Donaldson, *Analysis of Arf GTP-binding protein function in cells.* Curr Protoc Cell Biol, 2010. **Chapter 3**: p. Unit 14 12 1-17.
40. Zhu, Y., L.M. Traub, and S. Kornfeld, *High-affinity binding of the AP-1 adaptor complex to trans-golgi network membranes devoid of mannose 6-phosphate receptors.* Mol Biol Cell, 1999. **10**(3): p. 537-49.
41. Nie, Z. and P.A. Randazzo, *Arf GAPs and membrane traffic.* J Cell Sci, 2006. **119**(Pt 7): p. 1203-11.
42. Randazzo, P.A. and D.S. Hirsch, *Arf GAPs: multifunctional proteins that regulate membrane traffic and actin remodelling.* Cell Signal, 2004. **16**(4): p. 401-13.
43. Bejjani, B.A. and L.G. Shaffer, *Application of array-based comparative genomic hybridization to clinical diagnostics.* J Mol Diagn, 2006. **8**(5): p. 528-33.
44. Bennabi, D., et al., *Psychomotor retardation in depression: a systematic review of diagnostic, pathophysiologic, and therapeutic implications.* Biomed Res Int, 2013. **2013**: p. 158746.
45. Rice S, S.J., *Understanding the molecular genetics of the tubular transport disorder cystinuria.* OA Nephrology, 2013. **1**(1).
46. Abicht A, M.J.S., Lochmüller H, *Congenital Myasthenic Syndromes*, G. [Internet], Editor. 2003 [updated 2012 Jun 28], Seattle: Seattle (WA): University of Washington.
47. Niederwieser, A., et al., *GTP cyclohydrolase I deficiency, a new enzyme defect causing hyperphenylalaninemia with neopterin, biopterin, dopamine, and serotonin deficiencies and muscular hypotonia.* Eur J Pediatr, 1984. **141**(4): p. 208-14.

48. Techakittiroj, C., Andersson, H., Jackson, K., Dvorak, C., Li, M., *A female infant with hypotonia, developmental delay,transitional hearing loss and 22q13.1 deletion.* world Journal of pediatrics, 2006. **2**.
49. Magen, S., et al., *Human calmodulin methyltransferase: expression, activity on calmodulin, and Hsp90 dependence.* PLoS One, 2012. **7**(12): p. e52425.
50. Hsueh, Y.P., *Calcium/calmodulin-dependent serine protein kinase and mental retardation.* Ann Neurol, 2009. **66**(4): p. 438-43.
51. Zaffanello, M., et al., *A sporadic case of cystinuria, respiratory chain and growth hormone deficiencies.* Pediatr Nephrol, 2003. **18**(8): p. 846-7.

# Supplementary data 1.

Table 4. Primers for deletion screening

| **Primers name** | **Forward primer** | **Reverse primer (5′ – 3′)** |
|---|---|---|
| C2Orf34 exon 1 | GGCAGGTAAGGGAGAACC | GAGGAGTGACCAGAGGCAAA |
| C2Orf34 exon 2 | AGGCAAAGAAAGGGAAACTGA | TATATTGGACCCATGCACCA |
| C2Orf34 intron 2a | GCCTTTTCTGACAGTATTTCACATT | CCTAAACCTTATTCAGTCACATTACA |
| C2Orf34 intron 2b | ATAGCAAGAATAATTTCCTGACATCTT | AGACTATTTCACATTCTCACTGGCTA |
| C2Orf34 intron 2c | GAGAAGGAGTCTCAATCTGTCACC | GCAGTAAGCTGAGAATGGGCTA |
| C2Orf34 intron 2d | CAGATGAGATTGTGCCACTGA | TGTAACATCCCCAGTGTCTATTTTT |
| C2Orf34 intron 2e | CTCCCATATTTCAACTTAATTCCAG | GAAGCAATTTAAAGCTTCCAGAATA |
| C2Orf34 intron 2f | TATCTGCCCCAATGACTCGT | TGAGGAACTTTGAGTTTCTTCCTAA |
| C2Orf34 intron 2g | GGTGCAGACATCCATTGAACT | AGTTTCCCACATCATTAAGTAATATCC |
| C2Orf34 intron 2h | GCCCTCACACTGCCTTTTC | AGAGAGACATCAGGGTCATGC |
| C2Orf34 intron 2i | GTGTGCAAGGGTCTTTTTCG | GTCCAGCAATCCACTACTTG |
| C2Orf34 intron 2j | TGGAAATTTTGCTGAATTCTTTT | TGTTTACCTCGACAACCCTAAAG |
| C2Orf34 intron 2k | CCTTTTTCCACCCCTTTAAGTT | AGATCAAAACTCACCAACCAACTA |
| C2Orf34 intron 2l | TGGGTTCTAGCTACCCAGTGA | GGACTCTGTGCAGACAACCTC |
| C2Orf34 exon 3 | GGATCCTTGAATGTTGAAGATGT | TTTCCTGTATTGTCAAAGCTGGT |
| SLC3A1 exon 1 | CAGTGGCTTCTGTGCTGGTG | GGGCAATGATGGCTATGGTG |
| SLC3A1 exon 2 | ATCGTCCCTTAAAGATTTCAGATATGG | TCAACTTCCCGGAAATCTTCAA |
| SLC3A1 exon 5 | CCAAGCATTTTGCTTCTTCATCT | TGTGAGCCAGAACCGTAAAATTT |
| SLC3A1 exon 6 | CGGAGCTGTACCATGACTTC | GGACAATGTCGTGCATTCC |
| SLC3A1 intron 6 (1500bp) | TCTAAATGGAGTGATGAGAATTGC | CTCGTTGACATCCATGAAGACT |
| SLC3A1 intron 6 (600bp) | TCACCTGACGGTGTTCGAG | GTTCTAGTAGAGGAGGGGTTTCG |
| SLC3A1 exon 7 | TGGGAACAGCGTGTATGAG | TCTGGCATGTTTTCCATCCA |
| SLC3A1 exon 9 | AAAGTCACCAATGCAGTGG | GCTTCAGAAAAACCAGCAT |
| Deletion B | CTCAAACCCATTGCCTTCAT | CCCAGAAATCATCCATCTG |
| PREPL exon 1 | CAGACTTCGGCTGGACTTGC | AAACCAGTGAAGGCAGGCC |
| PREPL exon 2 | AACTTTTTCCAGGATCTTCAGCC | CACTTTTTCAAATGCATCCATGTT |
| PREPL exon 5 | ACGAGGAAGATGAAGATGTTTTATTCT | CACCAAAAGTGGCTCGATATACG |
| PREPL exon 6 | ACAAAAGACAGTCGTTTCCTCACC | AGGGCTCAGGCCATCTATCA |
| PREPL exon 7 | CCCCTGCAATTATGAATTGGG | GATCCTTAAACATGTCCAAGTCTATCACT |
| PREPL exon 8 | TCCTTGGGCCTGTGGATTC | GGACGTATTGGAGAGCAAAGTTG |
| PREPL exon 9 | GCATACTGCCATGTTCGGTG | ACATCTCTCACAATGGTCTAGCACTTA |
| PREPL exon 11 | TGGATGTTCTCAACACCATGATG | CAGATGAAGGATTCCCCCATT |
| PREPL exon 12 | CGGGTACCTCTGAAAGGAATTG | TTCACCTGTGTCCTTAGCATGC |
| PREPL exon 13 | TCCAGGCTATCAGACCCCTAATAT | TGATAACATACCTTTTTGTGAGAATCCTC |
| PREPL exon 14 | GGAACTTGGACTTGACAGCACC | TCCCAGTTGAATGCAGTGTTTC |

# Auteursrechtelijke overeenkomst

Ik/wij verlenen het wereldwijde auteursrecht voor de ingediende eindverhandeling:
**The role of PREPL in Hypotonia-Cystinuria syndrome; Genetic and immunocytochemical studies**

Richting: **master in de biomedische wetenschappen-klinische moleculaire wetenschappen**
Jaar: **2014**

in alle mogelijke mediaformaten, - bestaande en in de toekomst te ontwikkelen - , aan de Universiteit Hasselt.

Niet tegenstaand deze toekenning van het auteursrecht aan de Universiteit Hasselt behoud ik als auteur het recht om de eindverhandeling, - in zijn geheel of gedeeltelijk -, vrij te reproduceren, (her)publiceren of distribueren zonder de toelating te moeten verkrijgen van de Universiteit Hasselt.

Ik bevestig dat de eindverhandeling mijn origineel werk is, en dat ik het recht heb om de rechten te verlenen die in deze overeenkomst worden beschreven. Ik verklaar tevens dat de eindverhandeling, naar mijn weten, het auteursrecht van anderen niet overtreedt.

Ik verklaar tevens dat ik voor het materiaal in de eindverhandeling dat beschermd wordt door het auteursrecht, de nodige toelatingen heb verkregen zodat ik deze ook aan de Universiteit Hasselt kan overdragen en dat dit duidelijk in de tekst en inhoud van de eindverhandeling werd genotificeerd.

Universiteit Hasselt zal mij als auteur(s) van de eindverhandeling identificeren en zal geen wijzigingen aanbrengen aan de eindverhandeling, uitgezonderd deze toegelaten door deze overeenkomst.

Voor akkoord,

**-, Adelia**

Datum: **10/06/2014**